Jour. Fac. Sci., Hokkaido Univ., Ser. IV,
vol. 21, no. 3, Aug., 1985, pp. 417-451.

Experimental study of the system $Mg_3Al_2Si_3O_{12}$-$Mg_3Cr_2Si_3O_{12}$ at high pressure and high temperature

by

Tetsuo Irifune*

(with 13 text-figures and 7 tables)

Abstract

Phase relation between pyrope $Mg_3Al_2Si_3O_{12}$ and knorringite $Mg_3Cr_2Si_3O_{12}$ is determined experimentally under high pressure and temperature condition. The solubility limit of the knorringite molecule expands with increasing pressure, and knorringite end member is stable at pressures higher than 105 kbar at 1200°C. A low pressure phase assemblage of garnet $_{s.s.}$ + pyroxene $_{s.s.}$ + spinel $_{s.s.}$ + quartz (coesite) appears on the pyrope-rich side, while this assemblage is replaced by that of garnet $_{s.s.}$ + pyroxene $_{s.s}$ + corundum $_{s.s.}$ on the knorringite-rich side at the pressures above ca. 67 kbar at 1200°C. Measurement of chemical compositions of these phases is carried out, and the distribution of Cr^{3+} among the coexisting phases is determined. As a result, it is confirmed that the Cr content of the garnet, as well as that of the spinel, is a useful indicator of the equilibrium pressure between spinel and garnet lherzolites.

Melting experiment is made for the pyrope end member and also for the garnet solid solution between pyrope and knorringite at high pressures. It is observed that Cr^{3+} strongly prefers the garnet to the melt at relatively low pressures. However, such a preference is almost absent at the higher pressures around 90 kbar. On the other hand, an anomalous change of the quenched phase from the garnet melt is observed at pressures around 70 kbar; the quench crystal changes from aluminous pyroxene with garnet stoichiometry to garnet at these pressures. Further, notable decrease in slope of the melting curve is observed for the pyrope end member at around this pressure. It is strongly suggested that these changes would be caused by a pressure-induced structural change, from pyroxene-like structure with tetrahedrally coordinated Al to garnet-like one in which every Al is in an octahedral site, in the pyrope melt at the pressures about 70 kbar. This interpretation is confirmed by the X-ray emission spectroscopic measurement, which shows structural similarity between pyrope glass and the quench crystal.

Origin of Cr-rich pyrope and distribution of Cr in the upper mantle are discussed on the basis of the present experimental results. The Cr-rich pyrope, which commonly occurs as an inclusion in diamond, is estimated to be formed as a residual crystal caused by partial melting of the mantle material at pressures corresponding to 120-240 km in depth. It is also suggested that the garnet would be almost a unique phase which accommodates Cr^{3+} in the upper mantle from ca. 600 km to ca. 100 km depth, above which Cr^{3+} would be accommodated mainly in spinel and pyroxene. However, the notably high concentration of Cr^{3+} observed in the garnet inclusions ($Cr/Cr+Al=0.2$-0.5) is considered to be a local phenomenon limited in the shallower horizons above ca. 240 km.

Introduction

Pyrope-rich garnet is an important constituent of ultramafic xenoliths, and it has been considered to be a major mineral of the upper mantle together with olivine and pyroxene. Recent studies of the garnet inclusions, both in natural diamonds and in xenoliths from kimberlites, show that they usually contain considerable amounts of Cr_2O_3 (Nixon and Hornung, 1968; Sobolev, 1974; Tsai et al., 1980); the maximum value of the Cr_2O_3 content is about 0.5 in terms of $Cr/Cr+Al$. Thus knorringite

Contribution from the Department of Geology and Mineralogy, Faculty of Science, Hokkaido University, No. 1855.

* Research School of Earth Sciences, Australian National University, Canberra ACT 2601 Australia

$Mg_3Cr_2Si_3O_{12}$ would be an important end member of the garnet of mantle origin, and its effect on the stability condition of the garnet should be clarified for detailed discussion of the mineral composition of the mantle.

Ringwood (1977) synthesized the garnets with several compositions between pyrope and knorringite, and confirmed that they formed a complete solid solution series at high pressure. Irifune et al. (1982) determined the stability field of the knorringite end member and that of the garnet solid solution, and showed that the solubility of the knorringite molecule in pyrope depended largely on the pressure. However, some ambiguity remained on the mineral assemblage of the lower pressure phase of the garnet solid solution and also on the compositions of these minerals in the low pressure phase.

The enrichment of Cr^{3+} in the pyrope-rich garnet has been a subject of discussion in relation to the mechanism of formation of natural diamonds and the chemical composition of the upper mantle (Sobolev, 1974; Ringwood, 1977; Harte et al., 1980). Mineral inclusions in natural diamonds usually have high values of $Mg/Mg+Ca+Fe$ and $Cr/Cr+Al$ compared with those in ultramafic xenoliths, and such refractory features of the inclusions are considered to suggest participation of partial melting in the formation of the diamonds (Harte et al., 1980). The enrichment of the knorringite molecule is also thought to be caused by the repeated fractional melting in the upper mantle (Irifune et al., 1982). However, there were scarecely data on the partitioning of Cr^{3+} between crystals and melts, except for those obtained at quite low pressures (Barmina et al., 1974; McKay and Weill, 1976; Huebner et al., 1976; Ringwood et al., 1976). In particular, at the high pressures under which the diamond crystallizes, there were essentially no data because of technical difficulty in both generation and measurement of high temperature under such pressures.

Recent pioneering works of Ohtani and his co-workers enabled to perform a melting experiment under the conditions up to 200 kbar and 2500°C. They clarified the melting relations of several mantle-constituting minerals such as fayalite Fe_2SiO_4, forsterite Mg_2SiO_4, ferrosilite $FeSiO_3$, and those in some binary systems relating to these components (Ohtani, 1979; Ohtani et al., 1982; Ohtani and Kumazawa, 1982). As one of the series of these investigations, the author and his co-workers have carried out a melting experiment of pyrope, and reported a preliminary result in Ohtani et al. (1981). Although the experimental data were insufficient at that time, they observed an anomalous change of the quench phase and the associated change in the slope of the melting curve, and pointed out a possibility of occurrence of a pressure-induced coordination change of Al in the pyrope melt.

According to the X-ray studies of silicate melt (glass), cations are coordinated with several oxygen ions in the melt just as in a crystalline phase, and the melt maintains a local arrangement of the ions in short range order (e.g., Stanworth, 1950). Thus the coordination number of oxygen around a cation can be defined and measured even in the silicate melts. Accordingly, the pressure-induced coordination change, which is generally observed for the crystalline phases at high pressures, is also expected to occur in the silicate melt as pointed out by Waff (1975). Although Kushiro (1976) suggested the occurrence of such a coordination change for aluminum in jadeite melt around

10 kbar, the possibility is discarded by recent Raman spectroscopic studies at least at the pressures up to 40 kbar (Sharma et al., 1979; Mysen et al., 1980). However, such a structural change of the silicate melt may occur at the pressures higher than 40 kbar.

The author reports here the results of the following experimental studies;

1) determination of the phase relation and the distribution of Cr among the coexisting phases in pyrope-knorringite system at high pressure,

2) determination of the melting relation of pyrope and that of the garnet solid solution between pyrope and knorringite at high pressure,

3) characterization of the quenched phases from the garnet melt and exploration of the structure of the melt under high pressure.

The author discusses origin of the Cr-rich pyrope and distribution of Cr in the upper mantle on the basis of these experimental data. Implications of mineral inclusions in natural diamonds are also discussed in the present paper.

Experimental technique

High pressure and temperature generation

Piston-cylinder apparatus

Tow types of high pressure apparatus were used properly according to the aimed pressure range. A piston-cylinder apparatus with a working dimension of 1.25 cm in diameter and 5.0 cm in length was used in experimental runs at the pressures below 40 kbar. Constitution of the high pressure cell was essentially the same as that of Hariya and Kennedy (1968). An improvement of the cell assembly was made to generate higher temperatures than those of previous studies; a thinner and smaller graphite heater used in the present study enabled to perform melting experiment up to 2000°C under high pressures.

Each experimental run was carried out using piston-in technique with a correction of minus 10% for the nominal pressure. The pressure value under high temperature was checked by the equilibrium pressure between quartz and coesite at 1200°C (Boyd, 1964). Temperature was measured by a Pt-Pt13%Rh thermocouple in a subsolidus run. A W-W26%Re thermocouple, instead of the Pt-Pt13%Rh one, was used for the melting experiment at higher temperatures. No correction was made for the pressure dependence of the e.m.f. of each thermocouple.

MA8 apparatus

The MA8 type apparatus was used in the runs above 40 kbar. It possessed eight cubic anvils each of which had a truncated edge of 8 mm, and was driven by a uniaxial press through the RH3 type guide blocks; the principle of pressure generation and the method of the practical operation were explained in detail in Kawai and Endo (1970) and Kumazawa et al. (1972). Semi-sintered MgO was used as a pressure medium, and pyrophyllite was used as a gasket that laterally supported the anvils.

Pressure was calibrated by the resistance changes associated with the transitions of Bi (I-II, 25.5; III-V, 77 kbar; Lloyd, 1971) and Ba (I-II, 55; II-III, 126 kbar; Akimoto

et al., 1975). The error of the generated pressure is believed to be within 5% of the nominal value based on the calibration as shown in Ohtani (1979). However, a certain degree of pressure decrease, which probably depends on both run duration and temperature, is suggested to occur during the run as discussed in Irifune and Hariya (1983).

Specifically pure graphite was used as a heating element under high pressure; the graphite heater concurrently served as a container of the sample. A rapid transition of the graphite to diamond, however, occurred at the pressures above 95 kbar at around 2000°C, and it hindered stable generation of high temperature. Although Ohtani (1979) confirmed usefulness of $LaCrO_3$ as the heating element at the higher pressures than 100 kbar, it sometimes showed an erratic behavior in high temperature generation. Therefore, the author limited the experimental pressure below 100 kbar at present and aimed at determining of the melting curve and the phase relation as accurately as possible. Temperature was measured by the W-W26%Re thermocouple, and monitored by a digital recording system equipped with a microcomputer.

Run temperature was corrected for the temperature increase at the truncated edges of a couple of opposed anvils; both ends of the thermocouple were connected to the truncated edges. Because temperature was raised quickly ($\sim$500°C/min.) to avoid contamination by the furnace and the thermocouple to the sample, the whole cell system did not attain to thermal equilibration during a run. Therefore, the temperature of the anvil edges increased gradually through a run as a function of the duration, even if the electric power was held constant at the desired temperature. The temperature of the "cold junction" sometimes went over 300°C in a few minutes for the runs around 2000°C. In order to subtract the effect of such a temperature increase at the cold junction of a thermocouple, the e.m.f.'s for both the sample and the anvil edge were monitored simultaneously, and the run temperature was evaluated by the sum of these two values. However, some degrees of the systematic error of the temperature would have remained, because we could not remove the effects of pressure on the e.m.f. of the thermocouple and also because there was usually a large temperature gradient in the furnace of the MA8 type apparatus. On the other hand, the apparent observational error caused by the fluctuation of the temperature was usually within 1% of the nominal value (see, Table 2).

Experimental methods

Experimental procedure

The synthetic pyrope and the garnet solid solutions between pyrope and knorringite were used as starting materials of the melting experiment. In order to remove influence of absorbed water on the melting, the starting material was heated in an oven at 150°C for a day immediately before the run.

Quenching method was employed to recover stable phases under the experimental conditions. Pressure was applied first, and then temperature was raised quickly to an aimed value. Run duration was usually a few hours for the subsolidus experiment ex-

cept for that at 1000°C; the longer duration up to 10 days was taken to promote the reaction at this temperature. On the other hand, the duration was limited within a few minutes for the melting experiment at the temperatures near and above 2000°C, because the reaction would be accomplished in such short time under these extremely high temperatures. The short duration is also favorable to avoid contamination by the capsule and the thermocouple. After being held at constant temperature for the desired duration, sample was quenched isobarically by turning off the electric power. The quench rates in the present high pressure apparatus were very large, and the sample was quenched to the temperatures around the room condition within a few seconds.

Identification of phases

There was usually a large temperature gradient in the furnace of the MA8 type apparatus. Therefore, the run product only around the hot junction of a thermocouple was picked up carefully under the microscope. The product was identified by the microscopic observation and also by an X-ray powder diffraction method. Thin sections were prepared for the products of some critical runs, and EPMA analysis was made together with the microscopic observation. Detection of a molten phase could be readily made by the texture of the run product under the microscope; when a sample was melted, glass and/or dendritic quench crystals appeared as the product. These quench phases were well distinguished from the recrystallized granular crystals without melting.

Measurement of X-ray emission band

In order to clarify the aluminum coordination of the garnet melt, an X-ray emission band was measured for the synthetic crystals and the quenched phases from the melt. It was carried out by utilizing a commercially available EPMA equipped with a PET crystal as a monochromator; the Rowlands circle of the crystal had a radius of 125 mm. The Al $K\beta$ band was selected for the measurement because of its high sensitivity to immediate environment of the aluminum atom. The operating voltage was fixed to 10 keV and the width of the receiving slit in front of the detector was 0.3 mm; these conditions brought about wavelength resolution and peak intensity high enough for the present purpose. Electron beam was defocused to 50μm in diameter, which is somewhat larger than that usually employed in ordinary compositional analysis, to avoid contamination on the surface of the sample during measurement. A thin section of the sample, which was coated by carbon after polish, was prepared for the measurement.

A step scanning method with an interval of 0.001 Å in wave length was employed in the measurement of the X-ray band. Intensity of the emitted X-ray was measured three times for 20 seconds at a wave length, and the averaged value was taken as the real intensity at each wave length. In order to calibrate the wave length, the peak position of $K\beta$ for aluminum metal (7.960 Å; Bearden, 1967) was measured immediately before and after the measurement of each sample. The observational error of the wave length

was estimated to be within a half of the interval of step scanning as shown in the previous evaluatin for the same method (Maruno and Fujii, 1970).

Subsolidus phase relation in the system $Mg_3Al_2Si_3O_{12}$-$Mg_3Cr_2Si_3O_{12}$ at high pressures

Phase relation

Experimental study on the phase relationships in the pyrope-knorringite system has been made by the author, and the results are already published in Irifune et al. (1982), Hariya et al. (1982), and Irifune and Hariya (1983). A summary of these results is presented below.

Text-fig. 1 shows the stability field of knorringite end member at high pressure. Details of the experimental conditions and results are listed in Irifune et al. (1982). As shown in Text-fig. 1, knorringite is stable only at higher pressures than ca. 100 kbar, and an assemblage of enstatite + eskolaite appears at the lower pressures. The boundary between garnet and the low pressure phase has a positive and steep slope of about 8°C/kbar.

A phase diagram of the pyrope-knorringite system at 1200°C is illustrated in Text-fig. 2, which is equivalent to Fig. 1 of Irifune and Hariya (1983). The equilibrium pressure between the garnet solid solution and the low pressure phases almost agrees with that calculated by Irifune et al. (1982), and it depends largely on content of Cr in the garnet. Text-fig. 2 shows that the low pressure phase assemblage of the garnet solid solution consisted of garnet, pyroxene, and corundum solid solutions for the compositions with larger values than 0.4 in terms of Cr/Cr + Al. In contrast with this result, the garnet decomposed to an assemblage of garnet $_{s.s.}$ + pyroxene $_{s.s.}$ + spinel $_{s.s.}$ + quartz (coesite) at the pressures below ca. 67 kbar on the pyrope-rich side.

Irifune and Hariya (1983) studied temperature dependency of the phase boundary between the garnet and the low pressure phases. They showed that the phase boundary

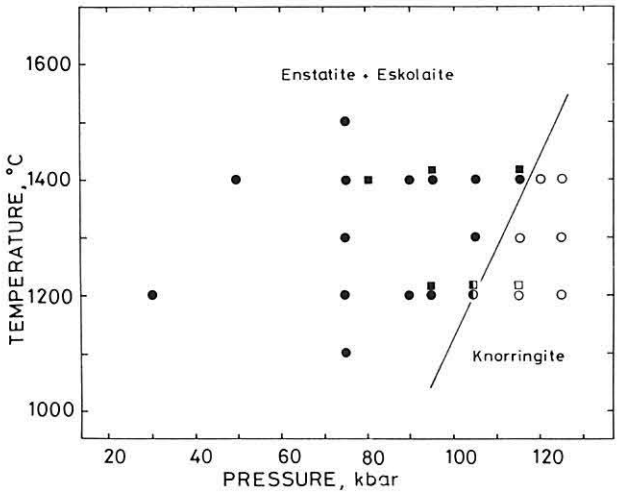

Text-fig. 1 Stability field of knorringite end member (after Irifune et al., 1982).

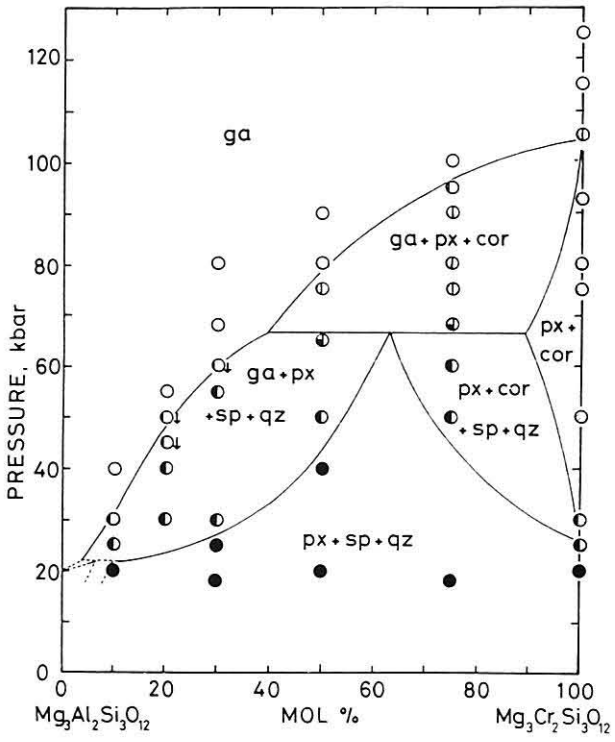

Text-fig. 2 Subsolidus phase relation between pyrope and knorringite at 1200°C (after Irifune and Hariya, 1983).

was raised to higher pressures with increasing temperature in the compositional range of the present study; this agrees with the temperature dependence of the phase boundaries for both pyrope and knorringite end members (Boyd and England, 1964; Irifune et al., 1982). However, the effect of temperature was not very large, and the slope of the phase boundary was in the order of 0.03 kbar/°C at each composition. Thus the solubility of the knorringite molecule in pyrope is dependent almost only on pressure, and it would become an indicator of the equilibrium pressure of natural garnet inclusions as discussed later.

Chemical compositions of crystalline phases

Compositional analysis was made by EPMA for the garnet solid solutions and the other crystalline phases which coexisted with the garnet under various pressures. Parts of the results are shown in Text-fig. 3 in terms of Cr/Cr + Al. Crystals of the spinel solid solutions were usually too minute to analyze accurately by EPMA. Therefore, the author determined chemical compositions of the spinel solid solutions by linear interpolation of lattice parameters of the end members following to the method by O'Neill (1981). One result of the EPMA analysis of a few exceptionally large spinel crystals obtained at 35 kbar showed the average composition of 0.63 in terms of Cr/Cr + Al, which almost agrees with the value (0.65) calculated from the lattice parameter. This

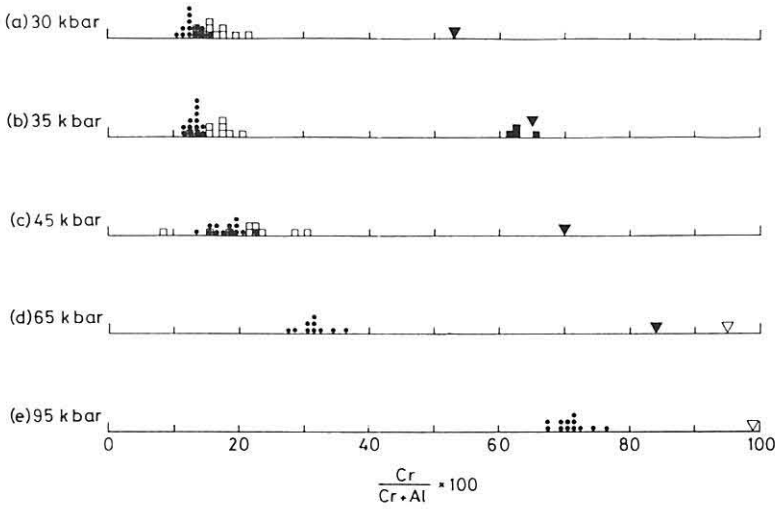

Text-fig. 3 Compositions of coexisting garnet and low pressure phases at 1200°C as a function of pressure. Circles and squares are results of EPMA analysis, and triangles are those based on lattice parameters. ●, garnet solid solution; □, orthopyroxene solid solution; ■, ▼, spinel solid solution; △, corundum solid solution.

suggests validity of the determination based on the lattice parameter.

The synthetic crystals obtained by the MA8 type apparatus showed considerable degrees of chemical inhomogeneity. In particular, orthopyroxene showed markedly large variation in $Cr/Cr+Al$ among the crystals synthesized in a run (see, Text-fig. 3). Therefore, the determination of its chemical composition with sufficient accuracy for a partitioning study of Cr^{3+} could not be made at present. Such a wide variation of $Cr/Cr+Al$ would be partly caused by analytical errors, because the contents of both Al_2O_3 and Cr_2O_3 in the pyroxene were extremely low under the pressures of the present study. The corundum solid solutions showed also erratic compositions and some of which were identified to be pure eskolaite by EPMA. Therefore, the average compositions for the corundum solid solutions were determined also by their lattice parameters.

Table 1 shows mole fractions of the Cr-components of the coexisting phases at various pressures at 1200°C. The additional data at 1000° and 1400°C and the apparent partition coefficient $K_{Cr\text{-}Al}$ between two major Cr-rich phases, spinel and garnet, are also shown in Table 1. Although these data are somewhat poor in quality at present, the order of partitioning of Cr^{3+} among the crystalline phases can be estimated from Text-fig. 3 and Table 1. The oxides such as corundum and spinel solid solutions have quite high Cr^{3+} preference rather than the silicates such as pyroxene and garnet solid solutions. Between the silicates, the orthopyroxene seems to have somewhat higher proportion of the Cr-component than that of the garnet solid solution, although the difference is not very large and is ambiguous especially at higher pressures. Similarly, the corundum solid solution has somewhat higher values of $Cr/Cr+Al$ than that of the

Table 1 Chemical compostions of the crystals in the assemblages of garnet $_{s.s.}$ + low pressure phases

Temp. (°C)	Press. (kbar)	X_{Cr}^{ga}	X_{Cr}^{sp}	X_{Cr}^{px}	X_{Cr}^{cor}	$K_{Cr\text{-}Al}^{sp\text{-}ga}$
1000	25	0.08	0.41	0.10	—	8.0
	30	0.12	0.59	0.14	—	10.6
	35	0.16	0.66	*	—	10.2
	40	0.20	0.75	*	—	12.0
1200	25	0.07	0.32	0.07	—	6.3
	30	0.12	0.53	0.15	—	8.3
	35	0.13	0.65	0.16	—	12.4
	40	0.16	0.69	0.18		11.7
	45	0.18	0.70	0.19	—	10.6
	55	0.25	0.78	*	—	10.6
	65	0.31	0.84	*	0.95	11.7
	80	0.52	—	*	0.98	
	95	0.71	—	*	0.99	
1400	30	0.07	0.43	0.06	—	10.0
	35	0.11	0.61	0.18	—	12.7
	50	0.19	0.67	*	—	8.7
	60	0.25	0.76	*	—	9.9

—, phase absent; *, Accurate determination could not be made.
X, mole fraction of Cr-component; K, apparent partition coefficient of Cr and Al.
Abbreviations: ga = garnet; sp = spinel; px = pyroxene; cor = corundum.

coexisting spinel solid slution as shown in Text-fig. 3 (d).

Melting relations in the system $Mg_3Al_2Si_3O_{12}$-$Mg_3Cr_2Si_3O_{12}$ at high pressures

Melting of pyrope at high pressures

Melting relation

Experimental conditions and the results of the melting of pyrope are summarized in Table 2 and Text-fig. 4. Pyrope melted congruently in the present pressure range between 35 and 95 kbar as shown in Text-fig. 4. The following changes of the quench phases were observed as a function of pressre: 1) At the pressures up to 55 kbar, glass of pyrope composition appeared together with quench crystals of aluminous enstatite, 2) the aluminous enstatite alone appeared as the quench phase in the pressure range between 55 and 70 kbar, 3) the quench crystal changed from the aluminous enstatite to pyrope at the pressures around 70 kbar, and the pyrope was the unique quench phase at the pressures beyond this. The apparent "phase boundary" between the these two quench crystals had a positive and very steep slope ($dT/dP = 35°C/kbar$) as shown by the dashed line in Text-fig. 4.

The slope of the melting curve of pyrope notably decreased at the pressures around 70 kbar, which corresponds to the pressure at which the quench crystal changed from

Table 2 Experimental conditions and results on melting of pyrope

Rur No.	Press. (kbar)	Temp. (°C)	Time (min.)	Apparatus	Results[a]
P1	35	1700 (10)[b]	5	PC	S
P2	35	1730 (5)	5	PC	S
P3	35	1750 (10)	7.5	PC	S + L (Gl, Q-En)
P4	35	1750 (20)	1.5	MA	L (Gl) + S
P5	35	1775 (10)	5	PC	L (Gl, Q-En) + S
P6	35	1800 (15)	3	MA	L (Gl, Q-En)
P7	50	1800 (15)	2	MA	S
P8	50	1850 (15)	2	MA	L (Gl, Q-En) + tr. S
P9	50	1875 (5)	3	MA	L (Gl, Q-En)
P10	50	1900 (30)	1.5	MA	L (Gl, Q-En)
P11	55	1850 (5)	2	MA	S
P12	55	1900 (10)	2	MA	L (Gl, Q-En) + S
P13	55	1930 (10)	2.5	MA	L (Gl, Q-En)
P14	62.5	1900 (10)	2	MA	S
P15	62.5	1950 (25)	1.5	MA	L (Q-En) + S
P16	62.5	1975 (10)	2	MA	L (Q-En, tr. Gl)
P17	62.5	c) 2100	—	MA	L (Q-En, tr. Gl)
P18	65	2050 (50)	0.1	MA	L (Q-En, tr. Gl)
P19	70	1950 (10)	2	MA	S
P20	70	1975 (5)	2.5	MA	L (Q-En)
P21	70	2000 (10)	2	MA	L (Q-En)
P22	70	2100 (50)	0.1	MA	L (Q-En)
P23	70	c) 2250	—	MA	L (Q-En)
P24	70	c) 2350	—	MA	L (Q-En)
P25	75	1950 (20)	3	MA	S
P26	75	2000 (10)	2.5	MA	L (Q-Py, tr. Q-En)
P27	75	2100 (15)	2.5	MA	L (Q-Py)
P28	75	2200 (15)	2.5	MA	L (Q-En)
P29	80	1950 (10)	2	MA	S
P30	80	2000 (10)	2	MA	S + L (Q-Py)
P31	80	2050 (10)	2	MA	L (Q-Py)
P32	80	2150 (50)	0.1	MA	L (Q-Py)
P33	80	2250 (25)	2.5	MA	L (Q-Py)
P34	80	2350 (15)	1.5	MA	L (Q-En, tr. Q-Py)
P35	85	1960 (5)	3	MA	S
P36	85	2000 (10)	2	MA	L (Q-Py) + S
P37	90	2000 (20)	2.5	MA	S
P38	90	2030 (15)	2	MA	L (Q-Py) + S
P39	90	2050 (15)	2	MA	L (Q-Py)
P40	90	2200 (50)	0.1	MA	L (Q-Py)
P41	95	2010 (15)	1.5	MA	S
P42	95	2040 (10)	2	MA	L (Q-Py) + S
P43	95	2075 (35)	1	MA	L (Q-Py)
P44	95	2250 (100)	0.2	MA	L (Q-Py)
P45	100	2075 (20)	0.5	MA	L (Q-Py)
P46	100	2150 (70)	0.1	MA	L (Q-Py)

[a]: Sequence of the phases follows their gross proportion in a run product.

[b]: Numeric values in parentheses in this column denote the observational error of temperature.

[c]: Sample was heated instantaneously, and the temperature was estimated from the supplied electric power.

Abbreviations: PC = piston-cylinder apparatus; MA = MA8 type apparatus; S = recrystallized pyrope without melting; L = phase recognized as being melted; Gl = glass; Q-En = quench aluminous enstatite; Q-Py = quench pyrope; tr. = trace.

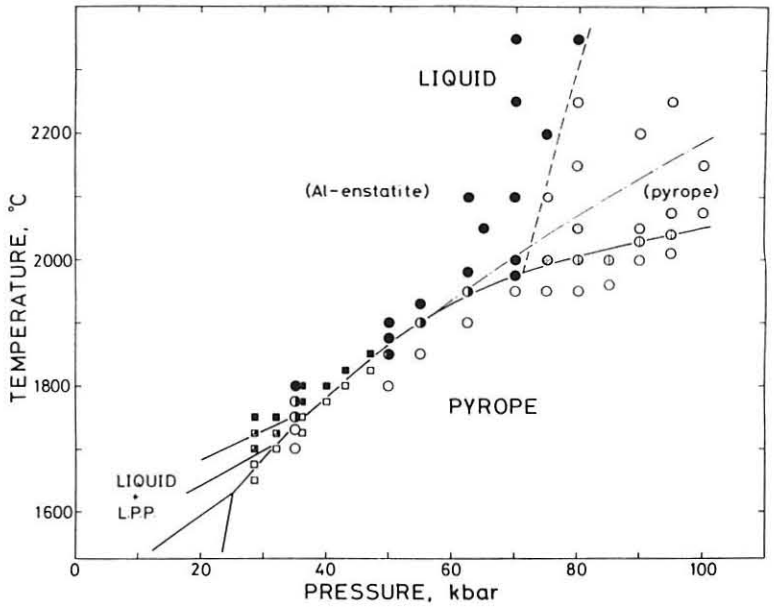

Text-fig. 4 Melting relation of pyrope up to 100 kbar. The dashed line indicates the apparent boundary between two quench crystals, aluminous enstatite and pyrope. The chain line is an extrapolated melting curve by the Kraut-Kennedy equation (see, text). Circles are the results of the present study, and squares are those by Boyd and England (1964).

aluminous enstatite to pyrope. The result of a detailed analysis of the melting curve is given in the next subsection.

Effect of pressure on the melting temperature

In the pressure range where pyrope melted congruently, the melting curve had a initial slope of about 8.2°C/kbar. However, the slope changed notably around 70 kbar as shown in Text-fig. 4. Such a bend of the melting curve was never observed in the previous experiments performed by essentially the same apparatus for other minerals such as fayalite and forsterite (Ohtani, 1979; Ohtani and Kumazawa, 1982), and the possibility that such a bend might be caused by inadequate estimation of the experimental pressure and/or temperature would be ruled out.

Slope of the melting curve of a solid usually decreases with increasing pressure, and such a tendency is well expressed by some empirical equations such as Kraut-Kennedy equation:

$$Tm = Tm_0 (1 + C (V_0\text{-}V)/V_0) \quad \ldots\ldots (1)$$

or $$Tm = Tm_0 + C' (V_0\text{-}V)/V_0 \quad \ldots\ldots (1')$$

where Tm and V are the milting temperature and the molar volume at pressure P, and Tm_0 and V_0 are those at the atmospheric pressue. C (C′) is a material-dependent constant which is determined by fitting the equation to the experimental data. The molar volume change at each pressure is evaluated by the third order Birch-Murnaghan equation of state;

$$P = 3/2K_0 ((V/V_0)^{-7/3} - (V/V_0)^{-5/3}) [1 + 3/4 (K'_0 - 4) \times ((V/V_0)^{-2/3} - 1)] \quad \ldots\ldots (2)$$

where K_0 is a bulk modulus at the atmospheric pressure, and K'_0 is its pressure derivative. Because pyrope is not stable at the atmospheric pressure, T_0 is not given experimentally.

Text-fig. 5 shows a relationship between the melting temperature and the molar volume change $1 - V_0/V$ of pyrope. The solid straight line was illustrated on the basis of a least squares fitting of the Kraut-Kennedy equation (1′) to the experimental data at the pressures less than 70 kbar. The experimental data used and the parameters thus obtained are shown in Table 3. The experimental data at the low pressures were best fitted to the equation $Tm = 1781 (1 + 7.2 (1 - V_0/V))$. However, the deviation of the experimental data from the solid line became very large at the larger values of $(V_0 - V)/V_0$ than 0.038 which corresponds to the volume change of pyrope at 70 kbar; these data are well described by the equation $Tm = 2027 (1 + 2.7 (1 - V_0/V))$ shown by the dashed line in Text-fig. 5.

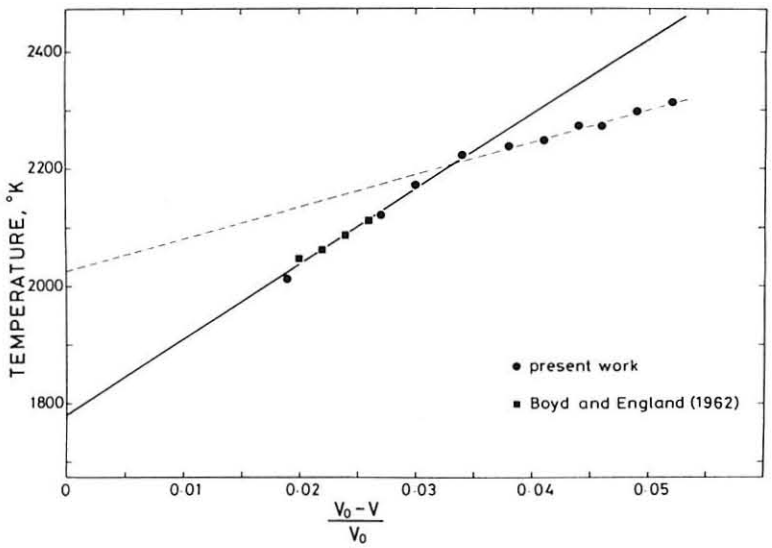

Text-fig. 5 Relation between the melting temperature and the volume change of pyrope. The solid line is illustrated by linear squares fitting of the present data below 70 kbar, and the dashed line is obtained by the fitting of the data at higher pressures.

Table 3 Experimental data used in the least squares fitting of Kraut-Kennedy equation and resultant parameters

Press. (kbar)	Tm (°K)	[a]$1-V/V_0$	Tm_0 (°K)	C
35	2023	0.019	1781[b]	7.2
[c]36	2048	0.020		
[c]40	2063	0.022		
[c]43	2088	0.022		
[c]47	2113	0.026		
50	2123	0.027		
55	2173	0.030		
62.5	2223	0.034		
70	2238	0.038	2027[b]	2.7
75	2248	0.041		
80	2273	0.044		
85	2273	0.046		
90	2298	0.049		
95	2313	0.052		

[a]: $K_0 = 1.71$ Mbar and $K_0' = 1.8$ (Sato et al, 1978) were used in the calculation.
[b]: These values are tentative ones,. because pyrope is not stable at the atmospheric pressure.
[c]: Boyd and England (1962).

The melting curve obtained by using (1′) and (2) is shown by the chain line in Text-fig. 4. It is shown that the change in the melting curve of pyrope can not be explained by the usual decrease in the slope of a melting curve at high pressure.

Melting of garnet solid solutions in pyrope-knorringite system at high pressures

Melting relation

Melting experiment of the garnet solid solutions in pyrope-knorringite system was carried out at the pressures 35, 62.5, and 90 kbar. The experimental conditions and results are summarized in Table 4. The experimental runs at 35 kbar were performed by the piston-cylinder apparatus, and those at higher pressures were made by the MA8 type apparatus. Chemical compositions of the garnets were limited to the pyrope-rich side in the present study. The results, however, would provide substantial information for the present purpose, because the natural garnets usually have the compositions 20-40% of the knorringite molecule and those with higher Cr contents than 40 mol % are extremely rare.

Text-fig. 6(a) shows the phase relation at 35 kbar. The garnet solid solution was stable in the compositional range of ca. 10% of Cr_2O_3 content. A small field of garnet s.s. + liquid existed near the pyrope end, which is shown by the region I in Text-fig. 6(a). Although this field was limited to the compositions below ca. 8% of the knorringite molecule and the accurate determination of the phase boundary could not be made, the shape of the field was estimated to be "fat" because of the high Cr/Cr + Al

Table 4 Experimental conditions and results on melting of garnet solid solutions between pyrope and knorringite

P = 35 kbar

Rur No.	Composition	Temp. (°C)	Time (min.)	Apparatus	Results[a)]
PK1	P95K5	1600 (10)[b)]	30	PC	Ga
PK2	P95K5	1700 (5)	10	PC	Ga
PK3	P95K5	1750 (5)	10	PC	Ga
PK4	P95K5	1800 (5)	10	PC	Ga + L (Gl, tr.Q-Px)
PK5	P95K5	1850 (15)	5	PC	L (Gl) + Sp + Px + tr.Ga
PK6	P95K5	1900 (10)	2	PC	L (Gl, tr.Q-Px)
PK7	P90K10	1600 (5)	15	PC	Ga + Sp + Px
PK8	P90K10	1805 (15)	2	PC	Ga + Sp + Px + tr.L (GL)

P = 62.5 kbar

Rur No.	Composition	Temp. (°C)	Time (min.)	Apparatus	Results[a)]
PK9	P90K10	1600 (15)[b)]	30	MA	Ga
PK10	P90K10	1900 (10)	2	MA	Ga
PK11	P90K10	1940 (10)	2	MA	Ga + (Q-Px)
PK12	P90K10	1975 (10)	1.5	MA	L (Q-Px) + tr.Ga
PK13	P90K10	2015 (10)	2	MA	L (Q-Px)
PK14	P80K20	1400 (10)	30	MA	Ga
PK15	P80K20	1600 (10)	25	MA	Ga
PK16	P80K20	1900 (15)	2	MA	Ga
PK17	P80K20	2000 (10)	2	MA	L (Q-Px) + tr. (Ga, Sp)
PK18	P80K20	2095 (10)	1.5	MA	L (Q-Px)
PK19	P70K30	1400 (10)	60	MA	Ga + Sp + Px
PK20	P70K30	1600 (25)	20	MA	Ga + Sp + Px

P = 90 kbar

Rur No.	Composition	Temp. (°C)	Time (min.)	Apparatus	Results[a)]
PK21	P95K5	2000 (10)[b)]	2	MA	Ga
PK22	P95K5	2050 (5)	1.5	MA	L (Q-Ga)
PK23	P90K10	2000 (10)	2.5	MA	Ga
PK24	P90K10	2050 (10)	2.5	MA	Ga + L (Q-Ga)
PK25	P90K10	2100 (15)	2	MA	L (Q-Ga)
PK26	P90K10	2200 (25)	1.5	MA	L (Q-Ga)
PK27	P80K20	2050 (20)	1.5	MA	Ga
PK28	P80K20	2120 (15)	2	MA	L (Q-Ga) + Ga
PK29	P80K20	2200 (20)	2	MA	L (Q-Ga)
PK30	P70K30	1900 (5)	15	MA	Ga
PK31	P70K30	2100 (5)	3	MA	Ga + L (Q-Ga)
PK32	P70K30	2160 (15)	2	MA	L (Q-Ga, Q-Px)
PK33	P70K30	2250 (30)	1.5	MA	L (Q-Ga, Q-Px)
PK34	P70K30	2400 (25)	1	MA	L (Q-Px, Q-Ga)
PK35	P60K40	2100 (15)	2	MA	Ga + tr. (Px, Cor, Sp)
PK36	P60K40	2260 (20)	2	MA	L (Q-Px)
PK37	P50K50	1600 (20)	20	MA	Ga + tr, (Px, Cor)
PK38	P50K50	1800 (15)	20	MA	Ga + Px + Cor

a), b): the same notations as in Tabel 2.

Abbreviations; P = pyrope; K = knorringite; Ga = garnet solid solution; Px = pyroxene solid solution; Cor = corundum solid solution; Sp = spinel solid solution; Q- = quenched crystal from melt; other abbreviations are the same as those in Table 2.

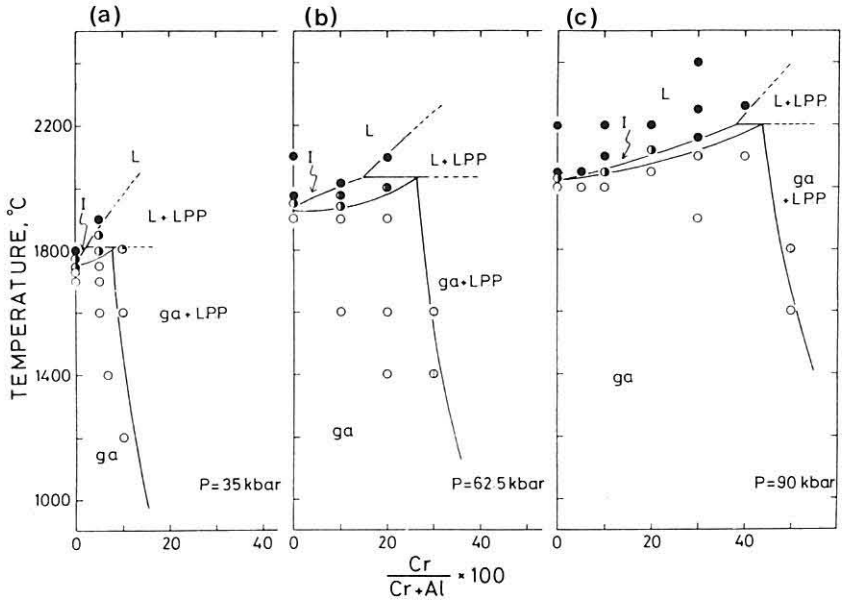

Text-fig. 6 Melting relation of garnet solid solution between pyrope and knorringite at (a) 35 kbar, (b) 62.5 kbar, and (c) 90 kbar. "I" indicates the field of garnet solid solution + liquid. L, liquid; ga, garnet solid solution; L.P.P., low pressure phases.

value of the garnet compared with that of the melt (see next section). The melt was quenched to the glass with a trace of quench crystals of orthopyroxene at this pressure. The liquidus and the solidus at the compositions of higher Cr/Cr + Al values are not determined at present, because they would be located at the extremely high temperatures beyond the potential of temperature generation of the present piston-cylinder apparatus and also because it is not the scope of the present study to clarify the partitioning of Cr^{3+} between melt and other phases except for garnet.

At 62.5 kbar, the stability field of the garnet solid solution expanded to the compositions up to ca. 30% of the knorringite molecule as shown in Text-fig. 6(b). The region of garnet $_{s.s.}$ + liquid also showed the fat shape suggesting that Cr^{3+} has still high preference for the garnet at 62.5 kbar. The quenched phase from the melt was always orthopyroxene with some amounts of Al_2O_3 and Cr_2O_3.

Further expansion of the stability field of the garnet solid solution was observed at 90 kbar as shown in Text-fig. 6(c). The field of garnet $_{s.s.}$ + liquid (region I) also expanded up to the composition with ca. 50% of the knorringite molecule. However, the compositional range of this region at a fixed temperature was considerably narrower than those of the regions at lower pressures. This indicates absence of the high concentration of Cr^{3+} in the garnet at the pressures around 90 kbar. The quenched phase from the melt was the garnet with a lamellar texture at the compositions within 20% of the knorringite molecule. However, the quench orthopyroxene coexisted with the quench garnet at the compositions with larger knorringite molecules.

Partition of Cr^{3+} between garnet and melt

EPMA analysis was made for the garnet and the glass (quench crystal) which coexisted in a run product at each pressure. The rsult is shown in Table 5. The author analyzed only one or two products for the starting compositions near the middle of the region I at each pressure, because the region of garnet $_{s.s.}$ + liquid was limited in a very narrow compositional range. Moreover, the products sometimes showed very large chemical inhomogeneity in terms of Cr/Cr+Al, and the average composition for several analytical points is shown for each sample in Table 5. The apparent partition coefficient $K^{Ga\text{-}L}_{Cr\text{-}Al}$ was calculated on the basis of the chemical analysis. The distribution coefficient of Cr^{3+} (D_{Cr} = wt% Cr in garnet/wt% Cr in melt), which is usually defined

Table 5 Chemical data of coexisting liquids and garnet solid solutions in pyrope-knorringite system

	P = 35 kbar (PK4)		P = 62.5 kbar (PK11)	
	garnet	liquid[a]	garnet	liquid[b]
SiO_2	43.84	43.91	43.74	44.81
Al_2O_3	23.06	24.03	21.41	23.52
Cr_2O_3	2.09	0.54	4.34	1.63
MgO	29.61	29.25	29.52	28.99
Total	98.60	97.73	99.01	98.95
Si	3.006	3.019	2.995	3.084
Al	1.862	1.914	1.768	1.926
Cr	0.114	0.030	0.238	0.089
Mg	3.025	2.998	3.054	2.974
Cr/Cr+Al	0.058	0.015	0.119	0.044
$K^{Ga\text{-}Lq}_{Cr\text{-}Al}$	4.0		2.9	
D_{Cr}	3.9		2.7	
	P = 90 kbar (PK24)		P = 90 kbar (PK28)	
	garnet	liquid[c]	garnet	liquid[c]
SiO_2	43.21	44.11	43.87	44.24
Al_2O_3	21.66	22.65	19.29	20.57
Cr_2O_3	3.97	3.48	7.38	5.56
MgO	28.69	28.18	27.99	28.49
Total	97.63	98.42	98.42	98.87
Si	2.988	3.059	3.007	3.052
Al	1.766	1.849	1.586	1.673
Cr	0.217	0.191	0.408	0.313
Mg	2.964	2.907	2.910	2.931
Cr/Cr+Al	0.109	0.094	0.205	0.158
$K^{Ga\text{-}Lq}_{Cr\text{-}Al}$	1.2		1.4	
D_{Cr}	1.1		1.3	

[a]glass; [b]quench pyroxene; [c]quench garnet.

for minor elements, was also calculated. The results of the calculation were also shown in Table 5.

At 35 kbar, a partially melted product was obtained at 1700°C and at the starting composition of $Py_{95}Kn_5$; the recrystallized garnet coexisted with the glass in this product. A trace of quench pyroxene was also observed in the product, but its proportion was extremely small. Therefore, its effect on the composition of the melt was ignored. The recrystallized garnet was rich in Cr_2O_3 compared with the glass; the apparent partition coefficient and the distribution coefficient were $K_{Cr\text{-}Al}^{Ga\text{-}L}=4.0$ and $D_{Cr}=3.9$, respectively.

The run product at 1940°C at the starting composition of $Py_{90}Kn_{10}$ was analyzed for the partitioning study at 62.5 kbar. Quenched pyroxene coexisted with the recrystallized garnet, but is showed quite large chemical variations in terms of Cr/Cr+Al. The average compositions of these phases brought about $K_{Cr\text{-}Al}^{Ga\text{-}L}=2.9$ and $D_{Cr}=2.7$. Although these values are somewhat small compared with those at 35 kbar, the high concentration of Cr is also observed in the garnet relative to the melt at this pressure.

It was difficult to identify the recrystallized garnet which coexisted with the melt at 90 kbar, because there was no glass and the garnet was the major quenched crystal from the melt. The run products for the starting compositions of $Py_{90}Kn_{10}$ and $Py_{80}Kn_{20}$ were analyzed, becuase they showed a textural feature of partial melting; both garnets with the granular and the lamellar textures coexisted in the product, although the coexistence was observed in a limited part. There was little difference in Cr/Cr+Al values between the two garnets, but a little enrichment of Cr^{3+} was observed in the recrystallized garnet compared with the quenched one. Consequently, both the values of the apparent partition coefficient and the distribution coefficient of Cr^{3+} were evaluated to be 1.1-1.4 at 90 kbar, which are considerably lower than those at 35 and 62.5 kbar. This agrees with the feature of the phase diagram at 90 kbar; the field of garnet+liquid exhibits a slender shape at 90 kbar as shown by I in Text-fig. 6(c). The author discusses later the reason for the notable decrease in the partition coefficient of Cr^{3+} between the garnet and the melt at the pressures around 90 kbar.

Analyses of quenched phases from garnet melt

Characterization of quench crystals

The quench crystal from the pyrope melt was identified by microscopic observation and X-ray diffraction method as aluminous enstatite at the pressures below ca. 70 kbar. SEM image of this quench enstatite is shown in Text-fig. 7(a). The results of precise characterization of the aluminous enstatite are reported in Fujino et al. (1983) and Irifune and Ohtani (1984). A summary of the results is as follows: The quench aluminous enstatite contains about 25 mol % of Al_2O_3, which just corresponds to the value of pyrope itself. It was reported that the upper limit of the Al_2O_3 content in orthoenstatite was about 16 mol % (Boyd and England, 1964). Therefore, the aluminous enstatite with the pyrope composition is most Al-rich one among those so far reported,

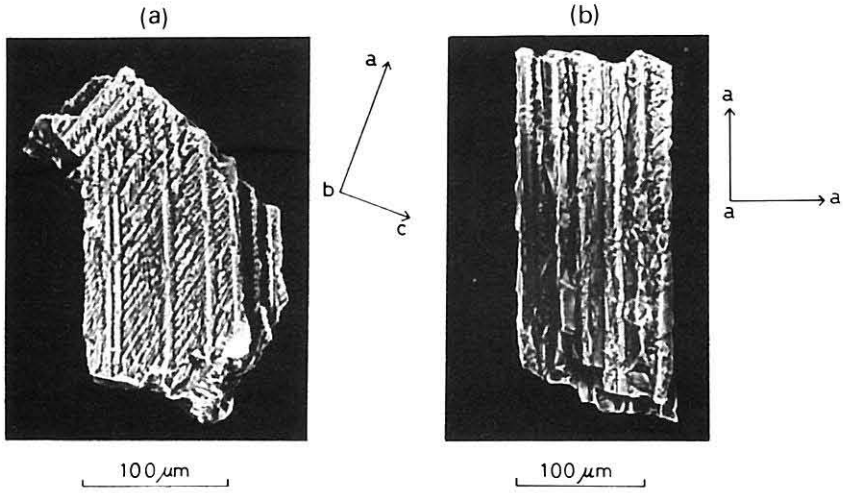

Text-fig. 7 SEM images of quench crystals from pyrope melt. (a) aluminous enstatite: The elongated direction of the lamellae disagrees with any axes; the included angle is 69.3° ± 0.5°. (b) pyrope: The crystal elongates in parallel with the a-axis.

although it might be a metastable phase.

At the higher pressures above 70 kbar, pyrope appeared as quench crystals from the melt. The chemical composition and the lattice parameter of the quench pyrope agreed with those of the synthetic one which was used as a starting material of the present experimental run. However, the quench pyrope exhibited a peculiar pillar shape as shown in Tex-fig. 7(b).

The variation of the quench crystal, from aluminous pyroxene to garnet with increasing pressure, was also observed in the melting experiment of the garnet solid solutions between pyrope and knorringite (see, next section) and of almandine $Fe_3Al_2Si_3O_{12}$ (Irifune, unpublished data). However, the "phase boundary" between the quench aluminous pyroxene and the quench garnet was raised to higher pressure with increasing knorringite molecule, and it shifted to a low pressure side for almandine compared with that of pyrope.

It is one of the subjects of the present investigation to clarify the reason why such a variation of the quench crystal occurs at high pressure. A reasonable explanation is that this variation is ascribed to a pressure-induced structural change in the garnet melt; if the garnet melt has a pyroxene-like structure with some of Al in a tetrahedral site at low pressures and a garnet-like structure with all Al in an octahedral site at higher pressures, the quench crystal from the melt would change according to the structural change of the melt. In order to examine this idea, the aluminum coordination in the pyrope melt was estimated on the basis of X-ray emission spectroscopic measurement.

Measurement of X-ray emission band for synthetic and quench phases

Principle and method of measurement

It is difficult to perform *in-situ* measurement of the structure of a silicate melt at high pressure. Recent study by a Raman spectroscopic method, however, shows that there is a similarity between a melt and the glass quenched from it (Seifert et al., 1981). It is also shown that the structure of a silicate melt at high pressure would be frozen by quenching. Therefore, analysis of the glass formed at high pressure will provide substantial information on the structure of a melt under compression.

There are several methods to analyze the structure of a glass as reviewed in Morikawa and Okuno (1983). The author selected an X-ray emission spectroscopic method, because it has the potential which directly clarifies the coordination of catins and also because it enables us to analyze such minute samples as are available in the high pressure experiment.

White and Gibbs (1969) studied the structural and the chemical effects on the X-ray emissioin bands for some aluminosilicates and oxides using a commercial EPMA. They found that the Al $K\beta$ band shifted as much as 8×10^{-3} Å and that the shift depended on both the coordination number of Al and the Al-O distance. Dodd and Glen (1970) and Maruno (1971) measured the Al $K\beta$ of various glasses which were obtained from the silicate melts under the atmospheric pressure. Both of them found that the position of the $K\beta$ band of a glass shifted to the high energy side compared with that of the corresponding cyrstal, which means that the strength of the M-O band in the crystal was weakened by the melting. However, they reported that there was no distinction between crystal and its melt (glass) in the coordination of cations; this agrees with the conclusions of the recent studies by several different methods (e.g.: Sharma et al., 1979; Okuno and Marumo, 1982). On the other hand, the measurement has never been made for the glass obtained at high pressure except for Velde and Kushiro (1978); their measurement seems quite poor in wave-length resolution of the X-ray band. Furthermore, little attention has been paid on the shift of the fine structure of the X-ray band in spite of its substantial importance in clarifying the coordination change.

In the present study, the AI $K\beta$ emission bands of synthetic aluminous enstatite, pyrope, and the quenched phases from the pyrope melt were measured by the method stated in the earlier section. The position and the full width at half peak height of the Al $K\beta$ were determined for each sample. Fine structure of the $K\beta$ was also analyzed by least squares curve fitting to evaluate the shift of the peak profile. The aluminum coordination numbers of the pyrope melt (glass) and the quench crystals were estimated by referring to these results for the synthetic aluminous enstatite and the synthetic pyrope, whose crystal structures have already been clarified.

Sample preparation

Measurement of the Al $K\beta$ band was made for the crystals and the glasses with pyrope composition. Synthetic conditions of the samples are shown in Table 6. Aluminous enstatite with 10 mol % of Al_2O_3 was also synthesized at high pressure to

Table 6 Synthetic conditions of samples with pyrope composition and results of measurement of Al K_β

Run No.	Sample name	Press. (kbar)	Temp. (°C)	Al K_β (Å)	
				position	FWH
PX1	S-PYR	30	1300	7.9774	0.0282
P31	Q-PYR	80	2050	7.9772	0.0286
PX2	*S-EN	30	1400	7.9749	0.0260
P22	Q-EN	70	2100	7.9753	0.0264
P6	GL-a	35	1800	7.9748	0.0263
P13	GL-b	55	1930	7.9755	0.0266

*Composition: $MgSiO_3 \cdot O.1Al_2O_3$.

Abbreviations: FWH = full width at half maximum of the peak; S-PYR = synthetic pyrope; Q-PYR = quench pyrope; S-EN = synthetic aluminous enstatite; Q-EN = quench aluminous enstatite; GL = glass.

compare with the quenched aluminous enstatite with the pyrope composition.

Glasses were prepared at 35 and 55 kbar. Although a small quantity of the quench aluminous enstatite was observed in the peripheral part of the latter sample, the central part of the sample was confirmed to be sure glass by the microscopic observation. At the pressures above ca. 70 kbar, however, glass was unavailable in the present study; a trace of the glass was obtained up to 65 kbar by the extremely short period heating including an instantaneous one, but no glass was available at pressures higher than 65 kbar. Therefore, no information was obtained on the structure of the pyrope melt at the higher pressures where the quench pyrope crystallized from the melt.

Thin sections of the samples were prepared for the X-ray band measurement by EPMA. The thickness of the thin section was adjusted to the same order as that of the radius of the electron beam (50 μm).

Experimental results

The results of measurement of the peak position and the peak width of Al K_β are shown in Table 6. A least squares fitting by several gaussian curves was carried out for the normalized X-ray intensity of the Al K_β peak. In the present curve fitting, the author referred to the methods which were used in the Raman spectroscopic study by Mysen et al. (1982) and the Mössbauer spectroscopic study by Shinno and Maeda (1981). The number of the gaussian peaks was increased till the addition of a new peak resulted in no significant improvement in terms of χ^2 test; only two or three gaussian peaks brought about sufficient result in the present study. The result of the deconvolution for each sample is shown in Text-fig. 8(a-f) and summarized in Table 7.

Al K_β of the synthetic pyrope was well expressed by a super-position of three gaussian peaks as shown in Text-fig. 8(a). The largest peak at about 7.979 Å would be assigned to the transition 3p (σ) — 1s in the octahedrally coordinated aluminum in the pyrope. The associated small peak at the high energy side would be assigned to a transition which reflects the covalent character peculiar to those atoms with 6-fold coordina-

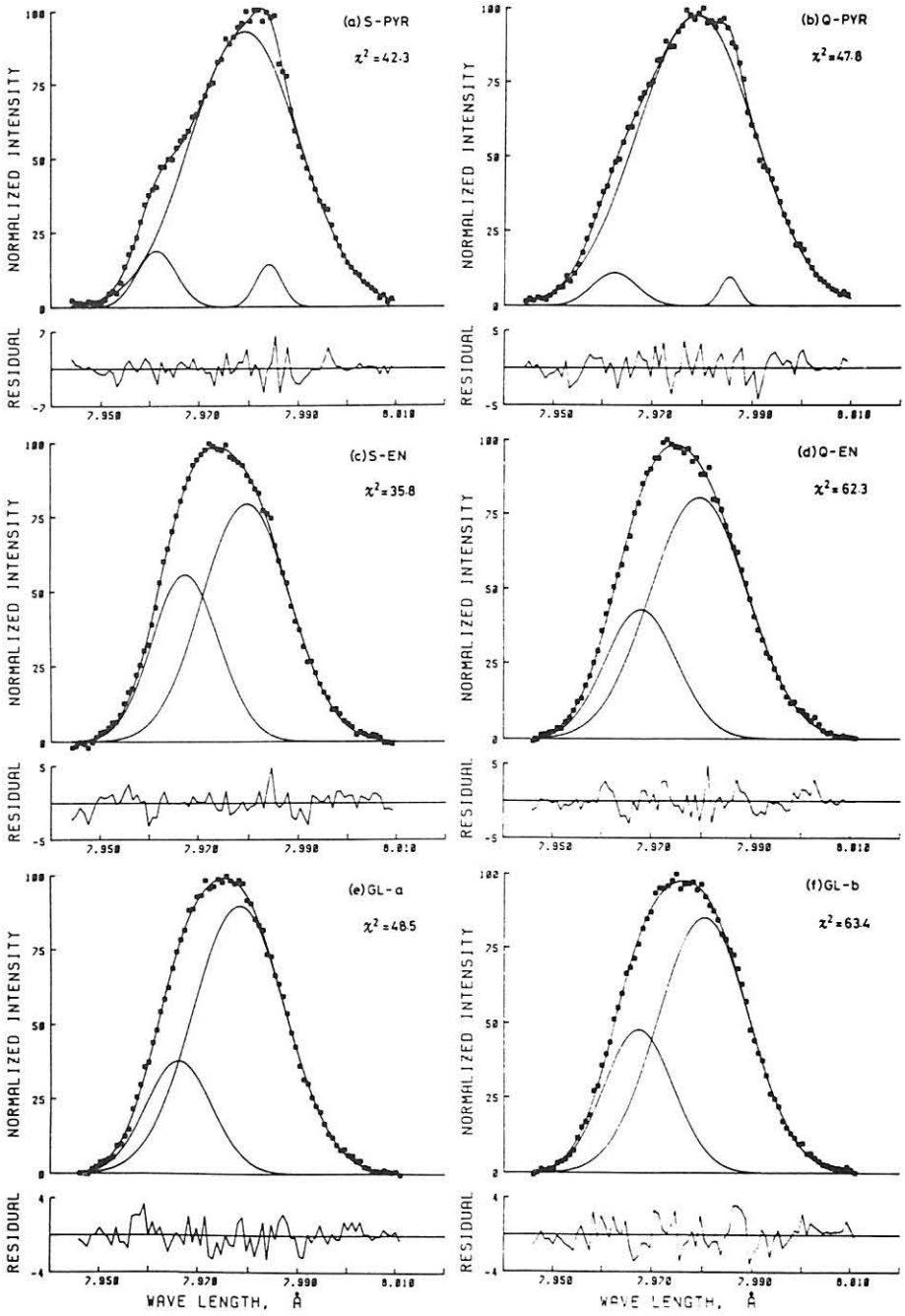

Text-fig. 8 Results of deconvolution for Al K_β bands of synthetic and quench phases. (a) synthetic pyrope; (b) quench pyrope; (c) Synthetic aluminous enstatite; (d) quench aluminous enstatite; (e) pyrope glass obtained at 35 kbar; (f) pyrope glass obtained at 55 kbar.

Table 7 Fine structure of the Al K_β band

Sample	PEAK 1*			PEAK 2			PEAK 3		
	P (Å)	F (Å)	I	P (Å)	F (Å)	I	P (Å)	F (Å)	I
S-PYR	7.9794	0.0257	93	7.9618	0.0095	19	7.9842	0.0062	14
Q-PYR	7.9786	0.0272	98	7.9623	0.0105	11	7.9854	0.0045	10
S-EN	7.9798	0.0205	79	7.9676	0.0157	56			
Q-EN	7.9794	0.0227	80	7.9679	0.0168	43			
GL-a	7.9783	0.0219	90	7.9660	0.0156	38			
GL-b	7.9803	0.0214	85	7.9674	0.0162	48			

*Peak number is assigned according to the normalized intensity of each elemental peak.
Abbreviations: P = position; F = full width at half maximum; I = normalized intensity.

tion; probably 3p (π^b) — 1s, according to an interpretation based on a molecular orbital theory (Glen and Dodd, 1968). As for the third minor peak around the main one, the assignment can not be made at present. It might reflect a 3s — 1s forbidden transition which is suggested to occur also in those atoms with 4-fold coordination (Dodd and Glen, 1968).

The Al K_β of the quench pyrope is shown in Text-fig. 8(b). There is no significant distinction of Al K_β in both the position and the profile between the synthetic pyrope and the quench one as noticed from Tables 6 and 7 and Text-fig. 8(a and b). Therefore, all of the aluminum atoms of the quench pyrope are considered to be in the octahedral site similar to those of the synthetic pyrope.

Text-fig. 8(c) shows the result for the synthetic aluminous enstatite with 10% of Al_2O_3. The Al K_β was decomposed to two gaussian peaks with similar intensity each other, and was very different from those of the synthetic and the quench pyropes in the peak position and the profile. According to the recent crystallographic study of synthetic and natural aluminous enstatites (Ganguly and Ghose, 1972), half of aluminum atoms occupy the tetrahedral B site and the remaining ones are accommodated in the octahedral sites, M1 and M2, with a preference for the M1 site. Therefore, the two elemental peaks of the Al K_β of the present synthetic enstatite are considered to be assigned to the electronic transitions in two kinds of the aluminum atoms with different coordination numbers. Since there is a tendency that the aluminum atom with a larger coordination number causes a shift of the K_β toward higher energy side (White and Gibbs, 1969), the two gaussian peaks around at 7.968 and 7.980 Å will be assigned to the transitions in octahedrally and tetrahedrally coordinated aluminum atoms, respectively. On the other hand, if these two peaks are assigned to those transitions, other minor peaks such as associated with the main peak of the K_β for pyrope Text-fig. 8(a and b) are expected to exist. However, the height of such peaks would be rather small (probably in the order of 10% of that of the main peak) according to the result for pyrope, and their presence was not confirmed in the present least squares analysis.

A similar result was obtained for the quench aluminous enstatite as shown in Text-fig. 8(d). Although the intensity of the high energy peak was somewhat weak com-

pared with that of the synthetic enstatite, the peak position and the profile of Al $K\beta$ of these enstatites almost agreed with each other. Thus the quench aluminous enstatite with pyrope composition is considered to be similar to the synthetic one in aluminum coordination; part of the Al would be in a tetrahedral site in these enstatites.

Text-fig. 8(e and f) shows the results for the glasses with pyrope composition obtained at 35 and 55 kbar, respectively. There was no significant distinction of Al $K\beta$ between these glasses, although the energy position of the Al $K\beta$ of the former glass was somewhat higher than that of the latter one. The Al $K\beta$ band of the glass shifted toward the high energy side compared with that of the crystalline pyrope, which implies that the Al-O bond strength was weakened by the melting. The profile of the Al $K\beta$ of the glass was also very different from that of the pyrope; only two gaussian peaks brought about a satisfactory result of the least squares fitting for the $K\beta$ of the glass. However, it is noteworthy that the position and the profile of the Al $K\beta$ of the pyrope glass almost agree with those of the quench aluminous enstatite as recognized from Table 6 and Text-fig. 8(c-f). The similarity between the glass and the aluminous enstatite is also confirmed by Text-fig. 9. Thus, at the pressures 35 and 55 kbar, pyrope melt is estimated to have the same aluminum coordination as that of the aluminous enstatite. Consequently, the occurrence of aluminous enstatite as the quench crystal is considered to reflect that the pyrope melt has the pyroxene-like structure, in which at least parts of the Al are tetrahedrally coordinated by oxygen atoms, at the low pressures below ca. 70 kbar.

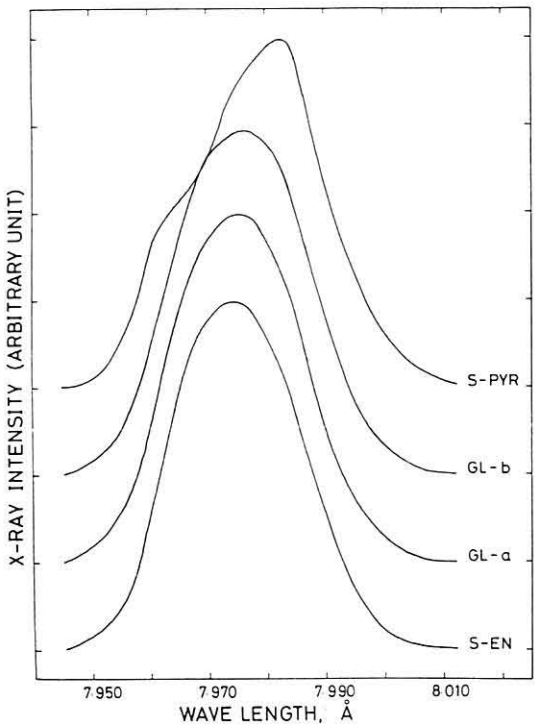

Text-fig. 9 Comparison of Al $K\beta$ bands between pyrope glasses and synthetic crystals. The profile of Al $K\beta$ band was illustrated on the basis of the results of curve fitting shown in Text-fig. 8.

Discussion

Effect of Cr on the transition pressure between spinel and garnet lherzolies

It is widely accepted that aluminous lherzolite constitutes a large part of the upper mantle, and many experimental studies have been carried out on the phase equilibrium between spinel and garnet lherzolites at high pressures (e.g.: MacGregor, 1975; O'Hara et al., 1971; Jenkins and Newton, 1979). As a result, the univariant phase boundary between two high pressure forms of the aluminous lherzolite was well determined for a simple model system of CaO-MaO-Al_2O_3-SiO_2 (abbreviated CMAS).

O'Neill (1981) discussed the effect of Cr_2O_3 on the phase transition of lherzolite on the basis of a high pressure experiment of the CMAS-Cr_2O_3 system up to 40 kbar. He showed that the addition of Cr_2O_3 to the CMAS system considerably raised the stability field of spinel lherzolite to higher pressures as shown by the chain line in Text-fig. 10, and found that the pressure at which an assemblage of five phases olivine + orthopyroxene + clinopyroxene + garnet + spinel appeared could be evaluated by the equation;

$$P = CX_{Cr}^{sp} + P_0 \qquad \ldots\ldots (3)$$

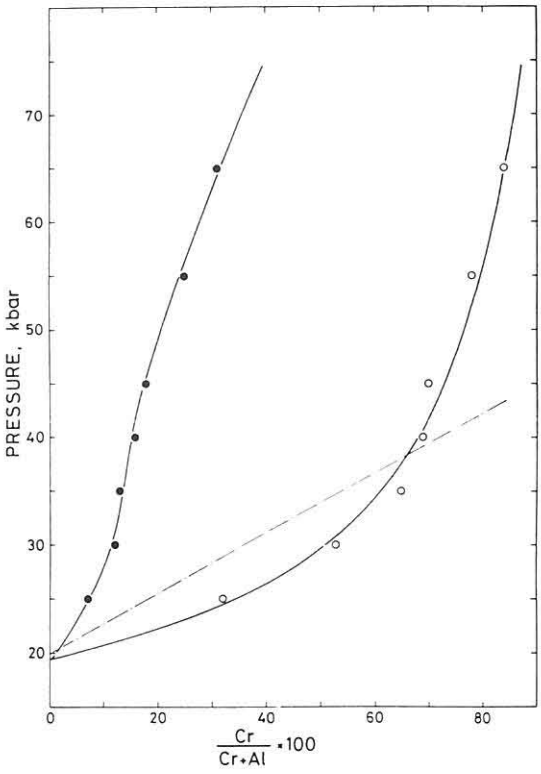

Text-fig. 10 Chemical compositions of coexisting spinel and garnet solid solutions at various pressures at 1200°C. Open circles are the results for the spinel, and closed ones are those for the garnet. The solid lines are to guide the reader's eye. The chain line is illustrated on the basis of the results for the spinel in CMAS-Cr_2O_3 system by O'Neill (1981).

where P_O is the equilibrium pressure of the univariant phase boundary between the spinel and the garnet lherzolites in the Cr_2O_3-free system, C is a constant with a value of 27.9 kbar, and X_{Cr} is the mole fraction of Cr in spinel. He applied this to several natural lherzolites and confirmed validity of its use as a geobarometer. However, as he mentioned in his paper, the linear equation (3) is merely empirical one which holds only in the pressure range covered by his experiment.

Text-fig. 10 also shows the result of the present chemical analysis of the spinel coexisting with the garnet in pyrope-knorringite system as a function of pressure (Table 1). It is shown that the pressure dependence of Cr contents in spinel is also well described by eq. (3) at the pressures less than 40 kbar, although the tentative value of P_O (= 16 kbar; obtained by regression of three data below 35 kbr at 1200°C) is somewhat lower than that obtained for the CMAS system (P_O/0 kbar). The systematic and small deviation of the present data from those for the CMAS-Cr_2O_3 system at the low pressure may be ascribed to some chemical effects which can not be evaluated at present. The present data, however, markedly deviated from the extrapolated values by eq. (3) with increasing pressure above 40 kbar. These results for the simple system between pyrope and knorringite indicate that the linear equation (3) may not be adequate for the relationship between the equilibrium pressure and the Cr content of spinel in the CMAS-Cr_2O_3 system at pressures higher than 40 kbar.

On the other hand, the author determined the composition of garnet solid solution in the assemblage of garnet + low pressure phases (spinel, pyroxene, and coesite) as shown in Text-fig. 10. It is noted that the Cr content of the garnet is also largely dependent on the pressure and that it changes almost linearly with increasing pressure in the pressure range up to about 70 kbar where the garnet coexisted with the spinel. Regression of the present data according to the linear equation (3) yields C = 150.0. This value is considerably larger than that for the spinel (C = 27.9), which suggests that the Cr content of garnet can be used as a geobarometer probably with greater potentiality than that of the "spinel geobarometer" at least in the ragne of relatively low pressure.

Text-fig. 11 shows the result of the application of present experimental data to several pairs of natural garnet and spinel from kimberlites. The equilibrium pressure for each sample was determined on the basis of Text-fig. 10. Temperature was assumed to be 1200°C, because the equilibrium temperatures of mantle xenoliths are usually in the range of 1100°-1300°C and the temperature effect on the Cr contents of garnet and spinel is not so large (Irifune and Hariya, 1983). As shown in Text-fig. 11, the correlation between the two pressure values for each pair is fairly good, although the pressure values obtained by the "spinel geobarometer" are generally somewhat larger than those by the "garnet geobarometer". Thus the Cr content of the garnet as well as that of the spinel in lherzolite is a useful indicator of the equilibrium pressure. However, it should be noted that these pressure values might not be exact ones, because the presence of other phases and components would somewhat affect the equilibrium pressures. Neverthless, such effects may not be very large as discussed later. It is noteworthy that Cr raises the equilibrium pressure between spinel and garnet lherzolites to extremely high pressures, and some lherzolites consist of the assemblages with

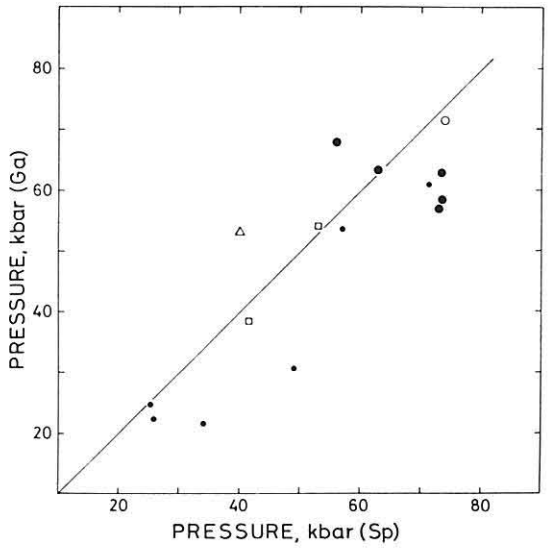

Text-fig. 11 Correlation between the equilibrium pressures obtained by the spinel and the garnet geobarometers (see, text). Data source: Sobolev (1974). ○, from diamond; •, from peridotite; ●, from garnet-pyroxene-chromite intergrowth; □, from porphyritic peridotites of the Udachnaya pipe; △, from pyrope peridotite of metamorphic complex.

coexisting spinel and garnet even at the high pressures around 70-80 kbar.

Chemical compositions of garnet inclusions from kimberlites are shown in terms of Fe/Fe+Mg and Ca/Ca+Mg versus Cr/Cr+Al in Text-fig. 12 on the basis of the re-

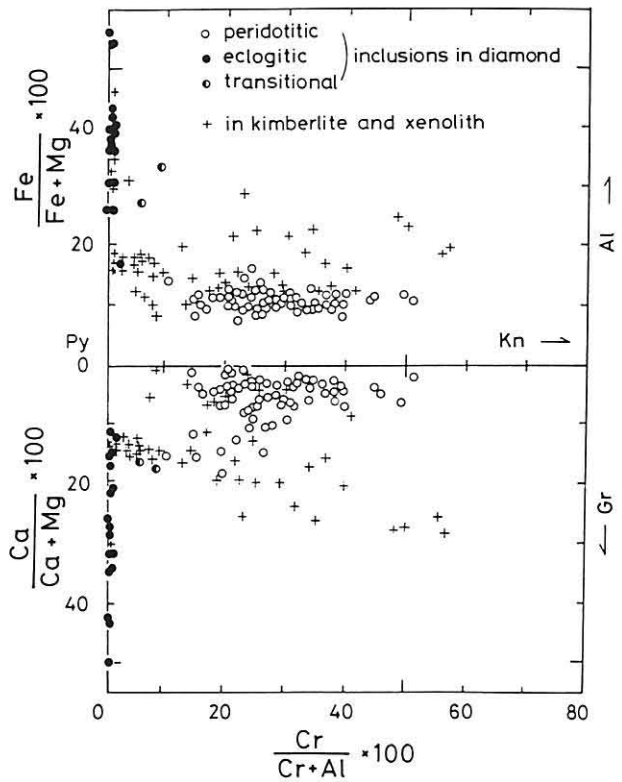

Text-fig. 12 Compositions of garnet inclusions in diamonds and those from kimberlites and associated xenoliths (after Irifune et al., 1982). Py, pyrope; Kn, knorringite; Al, almandine; Gr, grossular.

cent analyses by several authors (Sobolev, 1974; Tsai et al., 1979; Gurney et al., 1979). It is shown that most garnets of the peridotitic suite, especially those included in natural diamonds, have a compositional characteristic of extremely high Mg and Cr contents, and they are almost regarded as the solid solutions in the pyrope-knorringite system. Therefore, the lower limit of the equilibrium pressure of such a garnet can be estimated on the basis of the present experimental result on the stability field of the garnet solid solution.

As shown in Text-fig. 12, most garnet inclusions of the peridotitic suite have compositions of 0.15-0.5 in terms of Cr/Cr + Al with a strong concentration in the range 0.2-0.4. Such garnets are stable only at the pressure above ca. 40 kbar according to Text-fig. 2, and they are considered to be surely formed almost within the stability field of diamond. The maximum value of Cr/Cr + Al of the garnet inclusion is about 0.5 as shown in Text-fig. 12, which implies that it was formed at the pressures above ca. 80 kbar or at the depths below 240 km in the upper mantle (see, Tex-fig. 2). The depth is comparable to that of the peridotitic xenolith of the deepest origin in the upper mantle (Mercier and Carter, 1975).

Formation of mineral inclusions in natural diamonds

Recent vigorous studies on the mineral inclusions in natural diamond from various kimberlites have revealed their peculiarities in paragenesis and composition in comparison with those of xenoliths from the kimberlites. Since diamond crystallizes at the pressures corresponding to the depths below ca. 130 km and the effect of contamination or reaction by the wall rock and/or magma on the inclusion can be ignored in its ascending process, such an inclusion in the diamond is considered to provide us important information on the mineral assemblage and the composition of the upper mantle.

The mineral inclusions in natural diamonds can be classified into two types, peridotitic and eclogitic suites, according to their assemblages and chemical compositions (Sobolev, 1974). The peridotitic inclusions are usually predominant over the eclogitic ones, and they consist mainly of olivine, orthopyroxene and garnet. As shown in the previous section, most of the garnets in diamonds have peculiar compositions with notably high concentrations of Mg and Cr compared with the inclusions in ordinary peridotitic xenoliths. Other mineral inclusions in the diamonds also have refractory compositions with high Mg and Cr and low Ca, Fe, and Al contents. These compositional features of the mineral inclusions would hold the key to solve the problem of the formation of natural diamond and the inclusions themselves. Although it is not a scope of the present study to consider the process of the crystallization of a diamond itself, it is possible to estimate the environments under which the diamond crystallized together with these inclusions on the basis of the present experimental data.

The present experimental results on the melting of the garnet solid solutions between pyrope and knorringite showed a notably high preference of Cr^{3+} for the garnet rather than its melt at the pressures 35 and 62.5 kbar; the apparent partition coefficient between the garnet and the melt was in the order of 3-4. Therefore, effective concentra-

tion of Cr^{3+} in garnet is expected to be caused by partial melting of the mantle material. Moreover, the compositional features of the other mineral inclusions, such as olivine and pyroxene, also suggest the participation of the partial melting in their formations (Harte et al., 1980). On the other hand, there are several lines of evidence which indicate that natural diamonds crystallized in equilibrium with magmatic liquid (e.g., Fesq et al., 1975). Consequently, it is considered that the natural diamond would have nucleated in the melt, in which residual solid phases of Cr-pyrope, enstatite and olivine with extremely refractory compositions coexisted. Such residual minerals would have been incorporated into the diamond during its growth. Since the natural diamonds are commonly included in eclogitic xenolith, the melt in which they grew might be an eclogitic one, which is expected to be derived by partial melting of the upper mantle (Ringwood, 1958).

The peridotitic suite inclusions in diamonds are usually more refractory than those in ordinary peridotitic xenoliths, as shown above. This implies the occurrence of high degrees of partial melting in the upper mantle, although it might be a local phenomenon.

Distribution of Cr in the upper mantle

Text-fig. 13 shows distribution features of Cr and Al between garnet and other coexisting phases observed in the present experiment. It is roughly seen from Text-fig. 13 that the order of partitioning of Cr in these phases is corundum > spinel > pyroxene = garnet > melt. On the other hand, the partitioning of Cr as a minor element at

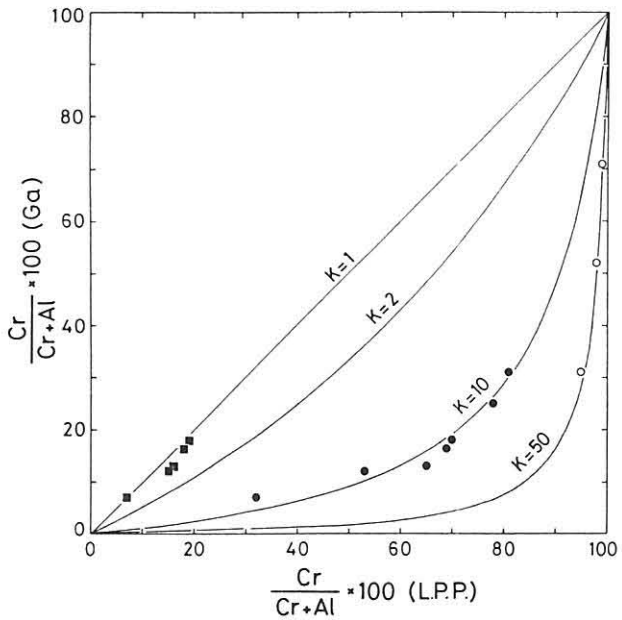

Text-fig. 13 Distribution features of Cr and Al between garnet and other low pressure phases (L.P.P.). K denotes the apparent partition coefficient. Data are those obtained in the present experiment for the pyrope-knorringite system. ●, garnet-spinel; ■, garnet-orthopyroxene; ○, garnet-corundum.

low oxygen fugacity shows the following order; pyroxene ≥ Ca-poor pyroxene > melt > olivine (Huebner et al., 1976). Moreover, the estimation based on the stabilization energies derived from crystal field spectra suggests the following sequence; spinel > garnet > pyroxene ≥ olivine (Burns, 1975). Being taken these results into consideration, the order of partitioning of trivalent chromium among major mantle-constituting minerals would be spinel > pyroxenes = garnet > melt > olivine, although some ambiguity remains on the partitioning between pyroxene and garnet.

Spinel and pyroxenes would be the major phases which accommodate Cr^{3+} at the shallower horizons of the upper mantle as expected from the above order. Indeed, the spinel from natural lherzolite is usually rich in the chromite molecule and pyroxenes have also a considerable quantity of Cr_2O_3. At the pressures around 30 kbar, however, spinel lherzolite with an ordinary amount of Cr_2O_3 ($Cr/Cr+Al=0.07$; Maaloe and Aoki, 1977) transforms to garnet lherzolite, and the garnet would be one of the major phases with high Cr_2O_3 contents at higher pressures than this. Although the pyroxenes have the same orders of Cr-components as that of the garnet, solubility of the traivalent cations in the pyroxenes is greatly limited by the pressure; the content of Cr_2O_3 is usually below 1 wt% for Ca-poor pyroxene which is the major phase of the pyroxene in garnet lherzolite. Further, the pyroxene with trivalent cations transforms to the garnet solid solution with a complex chemical composition (Ringwood, 1967; Akaogi and Akimoto, 1977). Therefore, garnet is considered to be almost unique phase which accommodates Cr^{3+} in the upper mantle below ca. 100 km depth. Such a situation would be held up to the depths around 600 km, below which the garnet transforms to pyroxenes with a perovskite-like structure through an ilmenite-like one (Liu, 1974, 1975). Since the trivalent cations would enter into the octahedral sites in the pyroxenes with the ilmenite-like and the perovskite-like structures, Cr^{3+} is expected to be incorporated into such pyroxenes at the depths below 600 km in the upper mantle.

The notable enrichment of Cr_2O_3 in garnet is considered to have been caused by the partial melting of mantle material as discussed in the previous section. However, such enrichment would not occur at the pressures above ca. 70-80 kbar, because the partition coefficient between the garnet and the magmatic liquid is expected to come close to unity on the analogy of the result for the garnet in the present study. As shown in Text-fig. 12, most garnets of the peridotitic suite have chemical compositions of the range $Cr/Cr+Al=0.2$-0.4, and the garnet with larger proportion of Cr than 0.4 is very rare. In addition, there have been no reports of Cr-rich pyrope with more than 50% of the knorringite molecule, which is stable only at the pressures above 80 kbar (see, Text-fig. 2). These compositional limits observed in the natural garnet inclusions are well explained by the change in the partitioning of Cr^{3+} between the garnet and the melt around 70-80 kbar, which is probably caused by the pressure-induced structural change in the melt. Thus the notable enrichment of knorringite molecule would be a local phenomenon limited in the depths above ca. 240 km, and the Cr-rich pyrope with more than 50% of the knorringite molecule may not be formed at any localities in the upper mantle.

Possibility of a pressure-induced structural change in garnet melt

It was confirmed on the basis of the X-ray emission band measurement that the pyrope melt (glass) obtained at the pressures 35 and 55 kbar is similar to the quench aluminous enstatite in the coordination of Al. The quench crystal changed into pyrope at the pressures above 70 kbar, and it seems reasonable to consider that such a change of the quench crystal was caused by a structural change of the pyrope melt, from pyroxene-like to garnet-like one, at high pressure. There is a body of additional evidence which supports this idea as discussed below.

The bend of the melting curve of pyrope around 70 kbar, which was shown in the previous section, indicates the presence of some structural changes in the crystalline pyrope and/or its melt. A pressure derivative of the melting temperature at pressure P is expressed by the Clausius-Clapeyron equation;

$$dTm/dP = \triangle V/\triangle S \qquad \ldots\ldots (4)$$

where $\triangle V$ and $\triangle S$ are differences of volume and entropy between a melt and a solid phase, and both values are usually positive if the values of volume and entropy of the solid are taken as standard ones. When an ordinary pressure-induced phase transition occurs in the solid phase, the slope of the melting curve changes abruptly at the pressure where the phase boundary encounters the liquidus. The slope of the melting curve usually increases discontinuously on the higher pressure side of the phase boundary, because the change of the volume difference in the phase transition of a solid is considerably larger than that of the entropy difference. Consequently, a sudden increase of dTm/dP occurs around the phase boundary, as is obviously seen from the eq. (4). However, the melting curve of pyrope shows the opposite shift of the slope, becoming smaller on the high pressure side beyond ca. 70 kbar. This suggests the occurrence of a "phase transition" on the very melt side.

On the other hand, the apparent "phase boundary" between the quench aluminous enstatite and the quench pyrope has a positive slope in the P-T diagram as shown in Text-fig. 4. Therefore, the value of entropy of the "high pressure phase" of the garnet melt would be lower than that of the "lower pressure phase" on the analogy of the entropy change associated with an ordinary first-order phase transition of a solid. This accords with the consideration that the pyrope melt would have pyroxene-like structure with both tetrahedrally and octahedrally coordinated Al at low pressures and garnet-like one with all Al in the octahedral site at the pressures above ca. 70 kbar.

Further, such a pressure-induced coordination change also explains the notable decrease in the partition coefficient of Cr^{3+} between the garnet solid solution and its melt as follows. Cr^{3+} usually prefers for an octahedral site to the tetrahedral one, because of high CFSE in the former site (Burns, 1975). This is the reason why the Cr^{3+} highly prefers for crystalline phases with octahedral sites relative to silicate melts in which most of the trivalent cations are considered to be tetrahedrally coordinated by oxygen atoms. In fact, the apparent partitioin coefficient of Cr^{3+} between the garnet

and its melt was very large (K = 3-4) at the pressures 35 and 62.5 kbar. However, the partition coefficient was evaluated as K = 1.3 at 90 kbar, which implies that the trivalent Cr is also octahedrally coordinated by oxygen atoms in the garnet melt as in the crystalline garnet under such a pressure. Thus the pressure-induced coordination change of trivalent cations in the garnet melt is also suggested to occur somewhere in the pressure range between 26.5 and 90 kbar.

All of these results obtained in the present experiment imply occurrence of the structural change of garnet melt at the pressures around 70 kbar. In order to positively conclude this, it is necessary to clarify the structure of the garnet melt (glass) obtained at the pressures above 70 kbar. Unfortunately, however, the glass has been unavailable at these pressures owing to rapid crystal growth in the garnet melt. The rapid crystal growth at such high pressures, being taken it the other way round, might be also caused by the structural change of the melt; the coordination change of Al would bring about depolymerization of the Si network of the melt, and it would cause certain degrees of viscosity decrease of the melt, which must promote crystallization of the quench phase.

Sharma et al. (1979) showed that there was no sign of occurrence of the pressure-induced structural change which was accompanied by a coordination change of cations in the melt at least at the pressures up to 40 kbar, although it has been suggested to occur on the analogy of the phase transition of a solid (Waff, 1976) and also on the basis of the measurement of physical properties of the melt (Kushiro, 1976; Velde and Kushiro, 1978). However, it is expected to occur at rather higher pressures around 70 kbar from the present experimental results. As the basaltic melts contain considerable amounts of Al_2O_3, such a structural change would have serious influence on physicochemical properties of the melts and, thereby, also on differentiation processes in the mantle.

Concluding remarks

It is shown that the stability field of Cr-rich pyrope expands to knorringite-rich side with increasing pressure, and the knorringite end member is stable at remarkably high pressures beyond 100 kbar. Compositional analysis of coexisting spinel and garnet in the pyrope-knorringite system yields a geobarometer which evaluates a pressure under which the Cr-rich pyrope equilibrated with low pressure phases. An estimation based on this barometer shown in Text-fig. 10 suggests that the peridotitic xenolith of deepest origin comes from ca. 240 km depth of the upper mantle. However, it should be noted that further study on partitioning of Cr between garnet and other phases to establish such a geobarometer with sufficient accuracy.

Present chemical analysis of coexisting garnet and melt indicates that Cr is strongly partitioned into the garnet relative to the melt. Thus pyrope-rich garnet with considerable amount of knorringite molecule must be a residual phase caused by partial melting of upper mantle material. The Cr preference for garnet is, however, not observered under the pressure of 90 kbar. Therefore, the notable enrichment of Cr in pyrope-rich garnet as a residual crystal must be limited within the uppermost horizons

(probably above ca. 240 km depth) of the mantle. Garnet, on the other hand, may be almost only phase that accommodates trivalent Cr above the seismic transition zone in the upper mantle, because there are essentially no other minerals which can accommodate this element in such a pressure range.

The present measurement of X-ry emission spectra for pyrope glasses shows that pyrope melt has a pyroxene-like structure in Al coordination at the pressures below 70 kbar. This yeilds aluminous enstatite as a quenched crystal from the pyrope melt at these pressures as observed in the present study. The change of the quench crystal, from aluminous pyroxene to garnet at ca. 70 kbar, is interpreted in terms of a pressure-induced Al coordination change of pyrope melt. Associated changes in the melting curve of pyrope and the partition coefficient of Cr between garnet and melt at around this pressure also favor the occurrence of the pressure-induced coordination change of cations in garnet melt. The pressure-induced cationic coordination change may also occur in magmatic liquids derived by partial melting of upper mantle. This must have serious influence on some physical properties of the melt such as density and viscosity, and also on partitioning of some minor elements between the melts and residual crystals.

Acknowledgements

The author expresses his sincere gratitude to Prof. Y. Hariya of Hokkaido University for his guidance and encouragement during this study. He also expresses his thanks to Prof. K. Togari of the same university for his useful suggestions and comments on the study. He is grateful to Prof. M. Kumazawa of Tokyo University and Prof. T. Yokokawa, Y. Katsui, and Dr. S. Dasgupta of Hokkaido University for their critical comments on the manuscript, and to Prof. S. Maruno of Nagoya Institute of Technology for his support in measurement of the X-ray emission band. He would like to thank Prof. H. Sawamoto and Dr. M. Kato of Nagoya University for their guidance in the initial stage of the present experiment and permitting the author to use the MA8 type high pressure apparatus of the same university. He also would like to thank Prof. K. Suwa of Nagoya University for his useful suggestions and comments on this study. Parts of the present experiments have been performed in cooperation with the following persons: Dr. M. Akasaka of Hokkaido University supported the author in preparation of starting materials and analyses of synthetic samples. Dr. Y. Oba and Mr. S. Terada of the same university technical supported him in high pressure experiment by a piston-cylinder apparatus. Dr. E. Ohtani and Prof. K. Fujino of Ehime University helped him in the characterization of quench crystals. Thin-section preparation of the run products were partly made by Mr. T. Kuwajima of Hokkaido University and Messrs. I. Hiraiwa and S. Yogo of Nagoya University. Mr. H. Ishiguro of Nagoya Institute of Technology helped the author in measurement of the X-ray emission band by EPMA. The author is sincerely grateful to all of the above persons. Parts of the numeric calculations in the present study were carried out with a FACOM-M200 at the Computation Center of Nagoya University (Problem No. KN2963).

References

Akaogi, M. and Akimoto, S., 1977. Pyroxene-garnet solid solution equilibria in the system $Mg_4Si_4O_{12}$-$Mg_3Al_2Si_3O_{12}$ and $Fe_4Si_4O_{12}$-$Fe_3Al_2Si_3O_{12}$ at high pressures and temperatures. *Phys. Earth Planet. Interior.*, 15: 90-106.

Akimoto, S., Yagi, T., Ida, Y., Inoue, K., and Sato, Y., 1975. High-pressure X-ray diffraction study on barium up to 130 kbar. *High Temp. — High Press.*, 7: 287-294.

Barmina, G.S., Yaroshevsky, A.A., and Shevaleyevsky, I.D., 1974. Partition of Si, Mg, Fe, Mn, Ca and Cr between olivine crystals and peridotite melt. *Geochem. Int.*, 11: 540-557.

Bearden, J.A., 1967. X-ray wavelength. *Rev. Mod. Phys.*, 39: 78-134.

Boyd, F.R., 1964. Geological aspect of high pressure research. *Science*, 145: 13-20.

Boyd, F.R. and England, J.L., 1962. Mantle minerals. *Carnegie Inst. Washington Yearb.*, 61: 107-112.

Boyd, F.R. and England, J.L., 1964. The system enstatite-pyrope. *Carnegie Inst. Washington Yearb.*, 63: 157-161.

Burns, R.G., 1975. Crystal field effects in chromium and its partitioning in the mantle. *Geochim. Cosmochim. Acta.*, 39: 857-864.

Dodd, C.G. and Glen, G.L., 1970. Studies of chemical bonding in glasses by X-ray emission spectroscopy. *J. Am. Ceram. Soc.*, 53: 322-325.

Fesq, H.W., Bibby, D.M., Erasmus, C.S., Kable, E.J., and Sellschop, J.P.F., 1975. A comparative trace element study of diamonds from Premier, Finsch and Jagersfontein mines, South Africa. *Phys. Chem. Earth*, 9: 817-836.

Fujino, K., Ohtani, E., and Irifune, T. 1983. Crystal chemistry of pyrope melts at high temperature and pressure and their quenched materials. *J. Mineral. Soc. Japan.* Special Vol. 1: 231-238.

Ganguly, J. and Ghose, S., 1979. Aluminuous orthopyroxene: order-disorder, thermodynamic properties, and petrologic implications. *Contrib. Mineral. Petrol.*, 69: 375-385.

Gibbs, G.V. and Smith, J.V., 1968. Refinement of the crystal structure of synthetic pyrope. *Am. Mineral.*, 50: 2023-2039.

Glen, G.L. and Dodd, C.G., 1969. Use of molecular orbital theory to interprete X-ray K-absorption spectral data. *J. Appl. Phys.*, 39: 5372-5377.

Gurney, J.J., Harris, J.W., and Rickard, R.S., 1979. Silicate and oxide inclusions in diamonds from Finsch kimberlite pipe. In: Boyd, F.R. and Meyer, H.O.A. (editors), *Kimberlites, Diatreams and Diamonds: Gheir Geology, Petrology and Geochemistry*. Am. Geophys. Union, Washington, DC., pp. 1-15.

Hariya, Y. and Kennedy, G.C., 1968. Equilibrium study of anorthite under high pressure and high temperature. *Amer. Jour. Sci.*, 266: 193-203.

Hariya, Y., Irifune, T., and Terada, S., 1982. Stability fields of chrome-pyrope and ferric iron-pyrope under upper mantle conditions. *J. Japan. Assoc. Min. Petr. Econ. Geol.*, Special Vol. 3: 203-206 (in Japanese).

Harte, B., Gurney, J.J., and Harris, W., 1980. The formation of peridotitic suite inclusions in diamonds. *Contrib. Mineral. Petrol.*, 72: 181-190.

Huebner, J.S., Lipin, B.R., and Wiggins, L.B., 1976. Partitioning of chromium between silicate crystals and melts. *Proc. 7th Lunar Sci. Conf.*, pp. 1195-1220.

Irifune, T., Ohtani, E., and Kumazawa, M., 1982. Stability field of knorringite $Mg_3Cr_2Si_3O_{12}$ at high pressure and its implication of the occurrence of Cr-rich pyrope in the upper mantle. *Phys. Earth Planet. Inter.*, 27: 263-272.

Irifune, T., and Hariya, T., 1983. Phase relationships in the system $Mg_3Al_2Si_3O_{12}$-$Mg_3Cr_2Si_3O_{12}$ at high pressure and some mineralogical properties of synthetic garnet solid solutions. *Mineral. J.*, 11: 269-281.

Irifune, T., and Ohtani, E., 1985. Melting of pyrope $Mg_3Al_2Si_3O_{12}$ up to 100 kbar: Possibility of a pressure-induced structural change in pyrope melt, *Proceeding of U.S. — Japan seminar on partial melting phenomena in the earth and planetary evolution* (in press).

Jenkins, D.M. and Newton, R.C., 1979. Experimental determination of the spinel peridotite to garnet peridotite inversion at 900 C and 1000 C in the system CaO-MgO-Al_2O_3-SiO_2, and at 900 C with natural garnet and olivine. *Contrib. Mineral. Petrol.*, 68: 407-419.

Kawai, N. and Endo, S., 1970. The generation of ultrahigh pressures by a split sphere apparatus. *Rev. Sci. Instrum.*, 41: 1178-1181.

Kumazawa, M., Masaki, K., Sawamoto, H., and Kato, M., 1972. Guide blocks and compressible pads for the practical operation of multiple-anvil sliding system for the production of high pressure. *High Temp. — High Press.*, 4: 293-310.

Kushiro, I., 1976. Changes in viscosity and structure of melt of $NaAlSi_2O_6$ composition at high pressures. *J. Geophys. Res.*, 81: 6347-6350.

Liu, L., 1974. Silicate perovskite from phase transformations of pyrope-garnet at high pressure and temperature. *Geophys. Res. Lett.*, 24: 224-228.

Liu, L., 1975. High-pressure reconnaissance investigation in the system $Mg_3Al_2Si_3O_{12}$-$Fe_3Al_2Si_3O_{12}$. *Earth Planet. Sci. Lett.*, 26: 425-433.

Lloyd, E.C., 1971. Accurate characterization of the high-pressure environment. *NBS Spec. Publ.* No. 326, Washington, DC., pp. 1-3.

MacGregor, I.D., 1965. Stability fields of spinel and garnet peridotites in the syntetic system MgO-CaO-Al_2O_3-SiO_2. *Carnegie Inst. Washington Yearb.*, 64: 126-134.

Maaløe, S. and Aoki, K., 1977. The major element composition of the upper mantle estimated from the composition of lherzolite. *Contrib. Mineral. Petrol.*, 63: 161-173.

Maruno, S. and Fujii, S., 1970. Measurements of aluminum X-ray emission bands shift by EPMA. *Japan. J. Appl. Phys.*, 9: 1428-1429.

Maruno, S. and Mitsuda, M., 1974. Studies of soda aluminosilicate glasses by X-ray emission spectroscopy. *Bulletin of Nagoya Institute of Technology*, 26, 197-203 (in Japanese).

McKay, G.A. and Weill, D.F., 1976. Application of major and trace element crystal/liquid partitioning to the origin of KREEP (abstract). In: *Lunar Science VII*, The Lunar Science Institute, Huston, pp. 527-529.

Mercier, J.G. and Carter, N.L., 1975. Pyroxene geotherm. *J. Geophys. Res.*, 80: 3349-3362.

Morikawa, H. and Okuno, M., 1983. Structural analysis of silicate melts and silicate glasses. *J. Mineral. Soc. Japan.*, Special Vol. 1: 123-136.

Mysen, B.O., Virgo, D., and Scarfe, C.M., 1980. Relations between the anionic structure and viscosity of silicate melts -A Raman spectroscopic study, *Am. Mineral.*, 65: 690-710.

Mysen, B.O., Finger, L.W., Virgo, D., and Seifert, F.A., 1982. Curve-fitting of Raman spectra of silicate glasses. *Am. Mineral.*, 67: 686-695.

Nixon, P.H. and Hornung, G., 1968. A new chromium garnet end member, knorringite, from kimberlite. *Am. Mineral.*, 53: 1833-1840.

O'Hara, M.J., Richardson, S.W., and Wilson, G., 1971. Garnet peridotite stability and occurrence in crust and mantle. *Contrib. Mineral. Petrol.*, 32: 48-68.

O'Neill, H.S.C., 1981. The transition between spinel lherzolite and garnet lherzolite, and its use as a geobarometer. *Contrib. Mineral. Petrol.*, 77: 185-194.

Ohtani, E., 1979. Melting of Fe_2SiO_4 up to about 200 kbar. *J. Phys. Earth.*, 27: 189-208.

Ohtani, E., Irifune, T., and Fujino, K., 1981. Fusion of pyrope at high pressures and rapid crystal growth from the pyrope melt. *Nature*, 294: 62-64.

Ohtani, E. and Kumazawa, M., 1981. Melting of forsterite Mg_2SiO_4 up to 15 GPa. *Phys. Earth Planet. Inter.*, 27: 32-38.

Ohtani, E., Kumazawa, M., Kato, T. and Irifune, T., 1982. Melting of various silicates at elevated pressures. In: Akimoto, S. and Manghnani, M.H. (editors) *Advances in Earth and Planetary Sciences*, 12, pp. 259-270.

Okuno, M. and Marumo, F., 1982. The structures of anorthite and albite melts. *Mineral. J.*, 11: 180-196.

Ringwood, A.E., 1958. Constitution of the mantle. *Geochim. Cosmochim. Acta*, 15: 195-212.

Ringwood, A.E., 1967. The pyroxene-garnt transformation in the earth's mantle. *Earth Planet. Sci. Lett.*, 2: 255-263.

Ringwood, A.E., 1976. Limits on the bulk composition of the moon. *Icarus*, 28: 325-349.

Ringwood, A.E., 1977. Synthesis of pyrope-knorringite solid solution series. *Earth Planet. Sci. Lett.*, 36: 443-448.

Sato, Y., Akaogi, M., and Akimoto, S., 1978. Hydrostatic compression of the synthetic garnets pyrope and almandine. *J. Geophys. Res.*, 83: 335-338.

Seifert, F.A., Mysen, B.O., and Virgo, D., 1981. Structural similarity of glass and melts relevant to petrological processes. *Geochim. Cosmochim. Acta*, 45: 1879-1884.

Sharma, S.V., Virgo, D., and Mysen, B.O., 1979. Raman study of the coordination of aluminum in jadeite melts as a function of pressure. *Am. Mineral.*, 64: 779-787.

Shinno, I. and Maeda, Y., 1981. A Fortran IV computer program LSF for analysis of Mössbauer spectra. *The Reports on Earth Science College of General Education, Kyushu Univ.*; 22, 13-26.

Sobolev, N.V., 1974. *Deep-seated inclusions in Kimberlites and the problem of the composition of the upper mantle*. Boyd, F.R. and Brown, D.A. (editors), Am. Geophys. Union, Washington D.C., 279 pp.

Stanworth, J.E., 1950. *Physical properties of glass*. Oxford Univ. Press, London, 360 pp.

Tsai, H., Meyer, H.O.A., Moreau, J., and Milledge, H.J, 1979. Mineral inclusions in diamond: Premier, Jagersfontein and Finsch kimberlites. In: Boyd, F.R. and Meyer, H.O.A. (editors), *Kimberlites, diatreams and diamonds: their geology, petrology and geochemistry*. Am. Geophys. Union, Washington, DC., pp. 16-26.

Velde, B. and Kushiro, I., 1978. Structure of sodium alumino-silicate melts quenched at high pressure; infrared and aluminum K-radiation data. *Earth Planet. Sci. Lett.*, 40: 137-140.

Waff, H.S., 1975. Pressure-induced coordination changes in magmatic liquids. *Geophys. Res. Lett.*, 2: 193-196.

White, E.W. and Gibbs, G.V., 1969. Structural and chemical effects on the Al K_β X-ray emission band among aluminum containing silicates and aluminum oxides. *Am. Mineral.*, 54: 931-936.

(Manuscript received on Apr. 3, 1985; and accepted on Apr. 23, 1985)